INVESTIGATIONS ON COMPOSITIONAL, STRUCTURAL AND OPTICAL PROPERTIES OF In_2S_3 FILMS PRODUCED BY SPRAY PYROLYSIS METHOD AT DIFFERENT SUBSTRATE TEMPERATURES

M. Sc. Thesis

in

Engineering Physics

University of Gaziantep

Supervisor

Assist. Prof. Dr. Metin BEDİR

by

Derya KORKMAZ

MAY 2008

T.C.
GAZİANTEP UNIVERSITY
GRADUATE SCHOOL OF
NATURAL & APPLIED SCIENCES
ENGINEERING PHYSICS GENERAL PHYSICS

Name of the thesis : Investigations on Compositional, Structural and Optical Properties of In_2S_3 Films Produced by Spray Pyrolysis Method at Different Substrate Temperatures

Name of the student : Derya KORKMAZ

Exam date : 30.05.2008

Approval of the Graduate School of Natural and Applied Sciences

Prof. Dr. Sadettin ÖZYAZICI
Director

I certify that this thesis satisfies all the requirements as a thesis for the degree of Master of Science.

Prof. Dr. Zihni ÖZTÜRK
Head of Department

This is to certify that we have read this thesis and that in our opinion it is fully adequate,in scope and quality, as a thesis for the degree of Master of Science.

Assist. Prof. Dr. Metin BEDİR
Supervisor

Examining Committee Members	Signature
Prof. Dr. Zihni ÖZTÜRK (Chairman)	______________________
Assoc. Prof. Dr. Mustafa ÖZTAŞ	______________________
Assoc. Prof. Dr. A. Necmeddin YAZICI	______________________
Assist. Prof. Dr. Bahattin KANBER	______________________
Assist. Prof. Dr. Metin BEDİR	______________________

ABSTRACT

INVESTIGATIONS ON COMPOSITIONAL, STRUCTURAL AND OPTICAL PROPERTIES OF In_2S_3 FILMS PRODUCED BY SPRAY PYROLYSIS METHOD AT DIFFERENT SUBSTRATE TEMPERATURES

KORKMAZ, Derya
M. Sc. in Engineering Physics

Supervisor: Assist. Prof. Dr. Metin BEDİR
May 2008, 79 pages

In this study, In_2S_3 films were prepared by spray pyrolysis technique and their compositional, structural, and optical properties were investigated by using different methods. The In_2S_3 films were obtained on glass substrates at various substrate temperatures in the range of 250-350 ºC. The compositional analysis of the chemicals was made by EDX method. The EDX results taken from an area on the film indicated that the film is composed of O, Na, and Si in small amounts, and also provided the ratio of the In (indium) to S (sulphur) on the film. The optical properties of In_2S_3 films were examined from optical absorption coefficient data using double beam visible spectrophotometer. The band gap energy of the In_2S_3 films was found to be between 2.61 eV and 2.71 eV. The crystal structure of the In_2S_3 film samples were studied by SEM and X-ray diffraction peaks. In addition, In_2S_3 films at different annealing temperature in O_2 flow were transformed into In_2O_3 films by thermal oxidation.

Key words: Spray pyrolysis technique, In_2S_3 films, compositional, structural and optical properties.

ÖZET

PÜSKÜRTME YÖNTEMİYLE ELDE EDİLMİŞ In_2S_3 FİLMLERİNİN FARKLI TABAN SICAKLIKLARINDA DÜZENSEL, YAPISAL VE OPTİKSEL ÖZELLİKLERİNİN İNCELENMESİ

KORKMAZ, Derya

Yüksek Lisans Tezi, Fizik Mühendisliği

Danışman: Yrd. Doç. Dr. Metin BEDİR

Mayıs 2008, 79 Sayfa

Bu çalışmada, In_2S_3 filmleri püskürtme yöntemiyle hazırlandı ve düzensel, yapısal ve optik özellikleri değişik yöntemler kullanılarak incelendi. In_2S_3 filmleri 250 ile 350 ºC arasında değişen farklı taban sıcaklıklarında cam zemin üzerine oluşturuldu. Kimyasalların düzensel incelemeleri EDX yöntemiyle yapıldı. Film üzerindeki bir alandan alınan EDX sonuçları, filmin az miktarda O, Na ve Si'den oluştuğunu ve ayrıca film üzerindeki In'nin S'ye olan oranını gösterdi. In_2S_3 filmlerinin optiksel özellikleri optik emilim katsayısı verilerinden çift ışınlı görünür spektrofotometre kullanılarak incelendi. Yasak bant enerjisinin 2.61 eV ile 2.71 eV arasında olduğu tespit edildi. In_2S_3 film örneklerinin kristal yapısı SEM ve X-ışını kırınım tepelerine bakılarak bulundu. Bunun yanısıra In_2S_3 filmleri O_2 ortamında farklı tavlama sıcaklıkları altında ısısal oksitleme ile In_2O_3 filmlerine dönüştürüldü.

Anahtar kelimeler: Püskürtme tekniği, In_2S_3 film, düzensel, yapısal ve optik özellikler.

ACKNOWLEDGEMENT

I would like to express my appreciation to my supervisor Assist. Prof. Dr. Metin BEDİR for his recommendation and help during the investigations, experiments, and preparation of this thesis. He conscientiously encouraged me throughout this work. Also I would like to thank to Assoc. Prof. Dr. Mustafa ÖZTAŞ for his suggestions.

I must acknowledge my colleagues Ebru BAKIR and Serap SÜR ÇELİK for their assistance and supportings. Also I would like to thank all of the Engineering Physics staff.

I would like to send my special thanks to my parents Hülya and Mehmet Ali, and all of my dear friends who are with me.

TABLE of CONTENTS

ABSTRACT iii

ÖZET iv

ACKNOWLEDGEMENT v

TABLE of CONTENTS vi

LIST of FIGURES ix

LIST of TABLES xi

CHAPTER 1. INTRODUCTION 1

CHAPTER 2. THEORY OF SEMICONDUCTORS 8

2.1 Equilibrium carrier concentrations and intrinsic material 11

2.2 Extrinsic Semiconductors 12

2.2.1 N-type Semiconductors 13

2.2.2 P-type Semiconductors 14

2.3 Band Gap of Semiconductors 16

2.3.1 Direct Gap Transition 17

2.3.2 Indirect Gap Transition 18

2.4 Absorption in Semiconductors 20

2.5 Band Theory of Solids and Semiconductors 21

2.6 Compound Semiconductors 23

2.6.1 III-VI Family Compound Semiconductors 25

2.6.1.1 In_2S_3 Semiconductors 26

2.7 Crystal Structure 27

2.7.1 Unit Cell 27

2.7.2 Crystal Lattice 28

2.7.3 **Crystal System** **29**
2.7.4 **Semiconductor Crystal** **30**

CHAPTER 3. **THIN FILM PRODUCTION TECHNIQUES** **32**
3.1 **Spray Pyrolysis Method** **32**
3.1.1 **Introduction** **32**
3.1.2 **Experimental Set-up of Spraying System** **32**
3.1.3 **Deposition Apparatus** **33**
3.2 **Growth Mechanism of The Semiconducting Films by The Spraying Pyrolysis Method** **34**
3.2.1 **Introduction** **34**
3.2.2 **Substrate Preparation** **34**
3.2.3 **Spraying Solution Preparation** **35**
3.2.4 **Development of In_2S_3 Films** **36**

CHAPTER 4. **MEASUREMENT METHODS** **37**
4.1 **Compositional Analysis** **37**
4.2 **X-ray Studies** **38**
4.3 **Optical Characterization** **39**
4.4 **SEM Analysis** **40**

CHAPTER 5. **RESULTS AND DISCUSSION** **42**
5.1 **Effect of The Substrate Temperature on The Film Formation** **42**
5.2 **Compositional Analysis** **42**

5.3 XRD Studies 43

5.4 Optical Characterization 48

5.5 SEM Analysis 50

5.6 Transformation from the In_2S_3 Film to In_2O_3 Film 54

CHAPTER 6. CONCLUSION 60

REFERENCES 62

PUBLICATIONS 68

LIST of FIGURES

page

Figure 2.1. Sketch of the conduction, forbidden, and valence bands within a semiconductor 9

Figure 2.2 Elements found in elemental and compound semiconductors. Group IV are elemental semiconductors. Compound semiconductors can be formed by combining Groups III and V or II and VI or III and VI 10

Figure 2.3. Intrinsic semiconductor 11

Figure 2.4. N-type semiconductor 13

Figure 2.5. N-doped material 14

Figure.2.6. P-type semiconductor 15

Figure 2.7. P-type material's energy bands 16

Figure 2.8. Band gap diagram of semiconductor 17

Figure 2.9. ($\Delta k = 0$) Change of electron momentum is zero. 18

Figure 2.10. ($\Delta k \neq 0$) Change of electron momentum is non zero 19

Figure 2.11. Model for light absorption. 20

Figure 2.12. Band diagrams for insulator, semiconductor, and conductor . . 21

Figure 2.13 Band diagram for a semiconductor, plotting E versus x 22

Figure 2.14 Dispersion diagram near the band edges 23

Figure 2.15 Periodic table for compound semiconductors 25

Figure 2.16 Unit cell 27

Figure 2.17 Crystal lattice 28

Figure 2.18 Crystal system 29

Figure 2.19 Semiconductor crystal 30

Figure 3.1 Schematic diagram of the spray pyrolysis system 33

Figure 3.2 Cleaning process of the glass substrate 35

Figure 5.1 EDX spectra of the In_2S_3 film prepared by spray pyrolysis 43

Figure 5.2 X-ray diffraction patterns of In_2S_3 films grown at different substrate temperatures, 200 ^oC, 250 ^oC, 300 ^oC and 380 ^oC . . . 44

Figure 5.3 Optical transmittance T(%) spectra of In_2S_3 films deposited at different temperatures 48

Figure 5.4 $(\alpha h\nu)^2$ versus $h\nu$ for In_2S_3 films deposited at different substrate temperatures, 250 ^oC, 300 ^oC and 350 ^oC 49

Figure 5.5 SEM image of In_2S_3 films at temperature
(a) 200 ºC 51
(b) 250 ºC 52
(c) 300 ºC 52
(d) 350 ºC 53

Figure 5.6 The XRD pattern of the as-deposited In_2S_3 films and the oxidized In_2O_3 films 55

Figure 5.7 Variation in crystallite size of the In_2O_3 films with respect to annealing temperatures 57

Figure 5.8 The plot of the $(\alpha h\nu)^2$ vs. the photon energy ($h\nu$) for (a) as-deposited In_2S_3 films and the oxidized In_2O_3 films at (b) 600 ^oC, (c) 800 ^oC 58

LIST of TABLES

		page
Table 2.1	Compound semiconductors	24
Table 5.1	Structural parameters of In_2S_3 films at various substrate temperatures	46

CHAPTER 1

1. LITERATURE SURVEY

Semiconductor crystals have recently been intensively investigated due to their novel properties that are markedly different from those of the bulk solids [1–3]. Among them, III–V group semiconductor nanocrystals, with more distinct quantum confinement effect, are likely to be the most promising candidates for fabricating nanoscale optoelectronic devices. GaP, with an indirect band gap at 2.26 eV, has been used in light emission devices in the visible range. Indium sulphide (In_2S_3) film is a technologically important transparent conducting material. It is used in different fields like: photovoltaic devices, transparent windows in liquid crystal displays, sensors, antireflection coatings [4], and electrochromic devices [5]. In_2S_3 films can be prepared by a variety of techniques such as chemical vapour deposition [6], spray pyrolysis [7], evaporation of indium followed by oxidation [8], vacuum evaporation [9] and magnetron sputtering [10]. Among these techniques, spray pyrolysis provides an easy route to fabricate films at low cost. It can be easily modified for mass production and device quality films can be obtained over a large area.

Recently, there has been increasing interest in III–VI materials, which have found applications in optoelectronic, photovoltaic industries [11] and photoelectrochemical solar cell devices [12]. Among these materials, In_2S_3 thin films appear to be promising candidates for many technological applications due to their stability [13], their band gap energy (2 eV) [14] and (2.8 eV) [15], their transparency and their photoconductor behavior [16]. These characteristics are suitable for application in solar energy conversion. Also, Indium Sulphide can be a binary base material in the deposition of semiconductor compounds such as In_2S_3; an absorber material in the hetero-junction of solar cell device structures [17].

In_2S_3 polycrystalline films with transmittance (70–80%) in the visible range can be used as an optical window in photovoltaic cells such us $In_2S_3/CuInX^2$ (X=S or Se). Indeed, it can constitute a good alternative to CdS layers [18]. It can also be used as an effective replacement for Cadmium Sulphide (CdS) in $Cu(In,Ga)Se_2$-based solar

cells. It is technically preferable to form the desired thin films by a simple and environment-friendly method. Thin films of In_2S_3 have been prepared by different methods such as: the photochemical deposition (PCD) technique [19], spray pyrolysis [20-21], atomic layer epitaxy [23], atomic layer deposition [24], reactive evaporation [25], thermal evaporation [26,27] and modulated flux deposition [28] .

In recent years, there has been a significant increase in the research works on III–VI materials, because of the enhanced interest due to their enhanced applications in optoelectronics and/or photovoltaic device fabrication [29]. Indium sulfide (In_2S_3) is a III–VI compound, originating from II–VI semiconductor, by replacing group II metals by group III elements [30]. Spray pyrolysis (SP) technique is one of the low cost techniques, which can be used to deposit large area thin films, and it is very cheap and simple. In_2S_3 is an interesting candidate with band gap between 2.0 and 2.45 eV, depending on thin film composition. The In_2S_3 buffer properties are strongly determined by the preparation procedure. Different methods are used in film preparation, like dry methods: spray pyrolysis [31], metal-organic chemical vapor deposition (MOCVD) [32] etc., and wet methods as chemical bath deposition (CBD) [33], electrodeposition [34]. Hence, the present investigation involves the study of the effect of thickness on physical properties such as structure changes, surface morphology and electrical properties of In_2S_3 films grown by spray pyrolysis at different thickness.

Spray pyrolysis involves the application of a fine mist of very small droplets containing the reactants onto the hot substrates in the atmospheric conditions. The critical operations of the spray pyrolysis technique are the preparation of uniform and fine droplets and the controlled thermal decomposition of these droplets. The In_2S_3 films were prepared by spraying an aqueous solution of $InCl_3$ and $(SC(NH_2)_2)$ on the high cleaned glass substrate kept at 350 ^oC. These samples are grown by a fine spray of the source solution using compressed air as a carrier gas. The atomization of the chemical solution into a spray of fine droplets is effected by the spray nozzle, with the help of compressed air by the air pump as carrier gas. Totally, 100 cm^3 of solution was used and sprayed different depositin time between 45 min and 4 hour. Details of the sample preparation are given elsewhere [35].

CSP is a very simple and low-cost technique, which could be used for deposition of large area thin films. The variation in band gap of β- In_2S_3 thin films, grown by spray pyrolysis, was studied by Kim et al.[36]. They also studied $Co_xIn_2S_{3+x}$ thin films having various compositions with x varying from 0.0 to 0.6 [37].

Photosensitivity of In_2S_3 films was found to vary with In/S ratio in the precursor solution by Teny et al. [38]. Bhira et al. also used this technique for the preparation of indium sulfide films to study structural and photoelectrical properties [39]. Optical properties of InS layers with In/S composition ratio varying from 0.4 to 0.6, deposited using an airless spray technique have been studied by Kamoun et al. [40]. They were also studied the effect of the nature of the substrate on β- In_2S_3 and introduction of small amounts of Al (β-$In_{2_x}Al_xS_3$) on the properties of the film [41]. Acoustic properties of indium sulfide thin films, prepared using the spray technique were also reported [42].

Indium sulfide could be used as an effective replacement for CdS in $CuInS_2$ based solar cells. The motivation of searching for an alternative buffer layer is not only to eliminate toxic cadmium but also to improve light transmission in the blue wavelength region, by using a material having a wider band gap, than CdS [43]. Indium sulfide thin films prepared using spray pyrolysis, with In/S ratio 2/3 in the solution, were annealed in vacuum at 300 and 400 °C by T.T. John et al [44]. The effect of this treatment on properties of the films was studied using X-ray diffraction, scanning electron microscopy, X-ray photoelectron spectroscopy, optical absorption, transmission and electrical measurements. Optical constants of the films were calculated using the envelope method. Annealing did not affect the optical properties of the film much, but the resistivity of the films showed a drastic decrease and the grain size increased. In_2S_3 thin films have potential use as buffer layer in photovoltaic heterojunction devices.

Indium sulphide, In_2S_3, thin films present an alternative to conventional CdS films as buffer layer for CIS-based thin film solar cells by A. Timoumi et al [45]. The objective is to eliminate toxic cadmium for environmental reasons. Indium sulphide is synthesized and deposited by single source vacuum thermal evaporation method on glass substrates. The films are analyzed by X-ray diffraction (XRD) and

spectrophotometric measurements. They have a good crystallinity, homogeneity and adhesion. The X-ray diffraction analysis confirmed the initial amorphous nature of the deposited InS film and phase transition into crystalline In_2S_3 formed upon annealing at free air for 250 °C substrate temperature for 2 h. The optical constants of the deposited films were obtained from the analysis of the experimental recorded transmission and reflectance spectral data over the wavelength range of 300–1800 nm. We note that the films annealed at 250 °C for 2 h show a good homogeneity with 80% transmission. An analysis of the optical absorption data of the deposited films revealed an optical direct band gap energy in the range of 2.0–2.2 eV.

β- In_2S_3 thin films, prepared using chemical spray pyrolysis technique, were irradiated using 100 MeV Au ions with different fluences by P. M. Ratheesh Kumar et al. [46]. Both unirradiated and irradiated samples were characterized using X-ray diffraction (XRD) techniques and optical absorption studies. XRD analysis showed that, on irradiation, crystallinity became poor. Mean crystallite size was calculated and it decreased from 17 nm to 10 nm as fluence increased up to 3 x 1012 ions/cm^2. XRD pattern revealed that, for ion fluence 1 x 1013 ions/cm^2, the sample became amorphous. However, when ion fluence increased to 3 x 1013 ions/cm^2, the grain size also increased to 16.5 nm, probably due to the recrystallization. A red shift in absorption edge was observed in the case of irradiated samples.

β- In_2S_3 thin films appear to be promising candidates for many technological applications due to stability, large band gap and photoconducting nature [47,48]. Chemical spray pyrolysis (CSP) technique is one of the low cost techniques, which can be used to deposit large area thin films, and it is very cheap and simple. In the present work CSP technique was used to deposit indium sulphide thin films. Swift heavy ion irradiation is a unique post deposition treatment, used to modify structural, optical and optoelectronic properties of thin film samples through the intense interaction of incident ions with the target atoms. There are several reports on structural and micro-structural phase transformation, due to irradiation using high-energy heavy ion in poly-crystalline and single crystal materials [49,50].

The crystal structure of annealed β- In_2S_3 thin films with different thickness was investigated by X-ray diffraction technique by M.M. El-Nahass et al [51]. Lattice

parameters, crystallite size and microstrain were calculated. It was found that the lattice parameters are independent on film thickness, while annealing temperatures increase them. Crystallite sizes were increased with the increase of the film thickness and improved by annealing temperatures. In all cases, the microstrains were decreased gradually with the increase in both film thickness and annealing temperatures. Optical properties of β- In_2S_3 thin films were performed in the spectral range from 400 to 2500 nm to determine the optical constants (n and k), the high frequency dielectric constant, ε_∞, the lattice dielectric constant, ε_L, and the energy gap. The optical constants were found to be independent on film thickness in the range from 200 to 630 nm. The high frequency dielectric and lattice dielectric constants of the as-deposited film increased by annealing temperatures. The energy gap for the as-deposited In_2S_3 was found to be 2.60 eV and increased to 2.70 and 2.75 eV by annealing at 423 and 473 K for 1 h, respectively.

They reported cubic structure with the preferential orientation (610). Powder neutron and XRD data on commercially indium sulfide were reported by Rampersadh et al. [57]. Their analysis was performed using Rietveld refinements and displayed the lattice parameters as: a=7.5937 Å, c=32.352 Å, V=1865.6 Å^3 in case of neutron diffraction and a=7.6172 Å, c=32.3307 Å, V=1875.86 Å^3 where XRD was used [52]. El- Shazly et al. [53] showed that the as-deposited In_2S_3 thin films were non-crystalline while they were found to have polycrystalline nature belonging to tetragonal β-phase after being annealed for 1 h at both 423 and 473 K. It was also found that the degree of crystallinity increases as the temperature of annealing increases. They found from both dark electrical resistivity and thermoelectric power of the as deposited and the after being annealed that In_2S_3 thin films were n-type semiconductors. Lokhande et al. [54] prepared γ- In_2S_3 thin film by chemical bath deposition and showed that the transition is direct with band gap of 2.75 eV. Sandoval-Paz et al. [55] prepared In_2S_3 thin films by the chemical bath deposition technique in an Ar atmosphere and temperature from 473 to 723 K. They showed mixture of cubic α and β crystalline phase with some fraction of tetragonal phase. Two energy band gaps were determined for all films: one indirect (2.12 eV) and the other direct (2.65 eV). These values were decreased for films annealed at 473–623 K and then increased for films annealed at 673–723 K.

It has been reported in the literature that thin films of β- In_2S_3 have their absorption edge mainly due to direct transition within the range of 2.0–2.9 eV [56,59]. The optical band gap of β-In_2S_3 containing different rates of sodium has been obtained by Barreau et al. [60] and found it linearly increases from 2.10 eV for pure β-In_2S_3 to 2.95 eV when sodium content was 0.9. Barreau et al. [61] showed that the optical energy gap of β-In_2S_3 containing oxygen with 8.5 at.% varied from 2.1 to 2.9 eV. John et al. [62] prepared thin films of β-In_2S_3 by chemical spray pyrolysis technique and obtained optical band gap, which has been decreased from 2.81 to 2.64 eV with In/S ratio varying from 2/1 to 2/8. Their samples were found suitable for any photovoltaic application. Choe et al. [63] studied the optical properties of β- In_2S_3 single crystal at 298 K and reported indirect and direct optical energy band gap as 2.24 and 2.64 eV, respectively. In order to obtain high band gap and low absorption material at low deposition temperature which is required for photovoltaic applications, Guilten et al. [64] prepared In_2S_3 thin films by novel modulated flux deposition procedure. Their results indicated that β- In_2S_3 has tetragonal structure with random or preferential (103) plane orientation. They also found that crystallite size decreased while the energy gap increased to value as large as 3.02 eV for the thinnest films.

There are several recent papers that report important advancements about the partial solution of this environmental problem [65–71]. For these reasons, it is important to investigate about other semiconductor materials with the appropriate properties to substitute the CdS buffer layer in the solar cell heterostructure. Several semiconductor materials have been investigated for the purpose of replacing the CdS buffer layer [72–73]. One of the most promising semiconductor materials studied is In_2S_3. There are reports about solar cells based on Cu(In,Ga)Se_2– In_2S_3 heterostructures that have achieved efficiencies as high as 15.7% [74,75]. Like CdS, In_2S_3 films can be prepared by the CBD method, keeping the possibility of large area deposition. Several crystalline phases have been reported for In_2S_3 films (a, h, and g) deposited by several techniques, with the tetragonal h phase being the most stable at room temperature.

This is the most common crystalline phase observed in In_2S_3 films [76–78]. The higher temperature cubic a phase has been observed in chemically deposited In_2S_3

films onto glass substrates as a mixture with the cubic h phase [79]. Amorphous In_2S_3 films onto glass substrates have also been obtained by the CBD method [80]. On the other hand, about the optical properties of In_2S_3 films, the energy band gap takes values between 2.0 and 2.75 eV, depending on the composition and deposition parameters [73,81]. There are reports on direct gap and indirect gap transitions. β-In_2S_3 films present a direct energy band gap with a value about 2 eV [77,79]. However, there are reports that this energy gap is indirect with a value about 2.2 eV [76].

Polycrystalline In_2S_3 films were grown on glass substrates by means of the chemical bath method and subsequently thermal-annealed in an Ar atmosphere at temperatures from 200 to 450 °C by M.G. Sandoval-Paz et al [65]. The optical and structural properties of the films were studied as a function of the annealing temperature. The experimental results show that the as- deposited films are composed by a mixture of both cubic α and β crystalline phases, with some fraction of tetragonal phase. The thermal annealing on the films produces the conversion of the cubic crystalline phases to the tetragonal β one and a crystalline reorientation of the latter phase. Two energy band gaps were determined for all the films: one indirect and other direct at higher energy. The structural modifications of the films are accompanied by changes in the two energy band gaps of the films.

A promising alternative buffer-layer material is indium sulphide, In_xS_y. For example, In_2S_3 is nontoxic, exhibits optical and electrical properties similar to those of CdS, and can be dry-deposited at low temperatures. It is an important material for photovoltaic applications [82], photoelectrochemical solar cell devices [83] and a promising candidate for many technological applications due to its stability, its interesting structural characteristics and optical properties [84]. The reported band gap values varies from 2.0 [85] to 3.3 eV [86] depending on the growth technique. In_2S_3 thin films were grown on glass substrates by means of the vacuum thermal evaporation technique and subsequently thermally annealed in nitrogen and free air atmosphere from 250 to 350 °C for different durations by A. Timoumi et al [87]. Experimental parameters have been adjusted in order to optimize the annealing conditions, and to obtain high band gap energy at low deposition temperature, as required for photovoltaic applications.

CHAPTER 2

2. THEORY OF SEMICONDUCTORS

Semiconductors are materials which have a conductivity between conductors (generally metals) and nonconductors or insulators (such as most ceramics). Semiconductors can be pure elements, such as silicon or germanium, or compounds such as gallium arsenide or cadmium selenide. Semiconductors are very similar to insulators. The two categories of solids disagree initially in that insulators have larger band gaps — energies that electrons must obtain to be free to move from atom to atom [88]. In semiconductors at room temperature, just as in insulators, very few electrons gain enough thermal energy to jump the band gap from the valence band to the conduction band, which is necessary for electrons to be available for electric current conduction. For this reason, pure semiconductors and insulators in the absence of applied electric fields, have roughly similar resistance. The smaller bandgaps of semiconductors, however, allow for other means besides temperature to control their electrical properties.

An entirely empty band cannot conduct a current. Since an empty band has no carriers within it and so there is nothing to carry the current. A completely filled energy band also cannot conduct a current. This is the fact that no two electrons can simultaneously occupy the same quantum state. The Pauli Principle has an importance in the formation of atoms [89].

Electrons within the conduction band can freely propagate through the crystal and so can carry a current. Electrons within the valence band are localized into bound electronic states formed by the molecular bonding of the constituent atoms of the crystal. In the forbidden band, no electronic states exist and thus electrons cannot exist within the forbidden band. The forbidden band is also said to be the energy gap.

An electron cannot move into an already occupied state according to the Pauli Principle. Electrons must move from one state to another for a current to flow. In a

filled band there are no vacancies into which the electrons can move since all possible states are filled. Therefore, no current can flow.

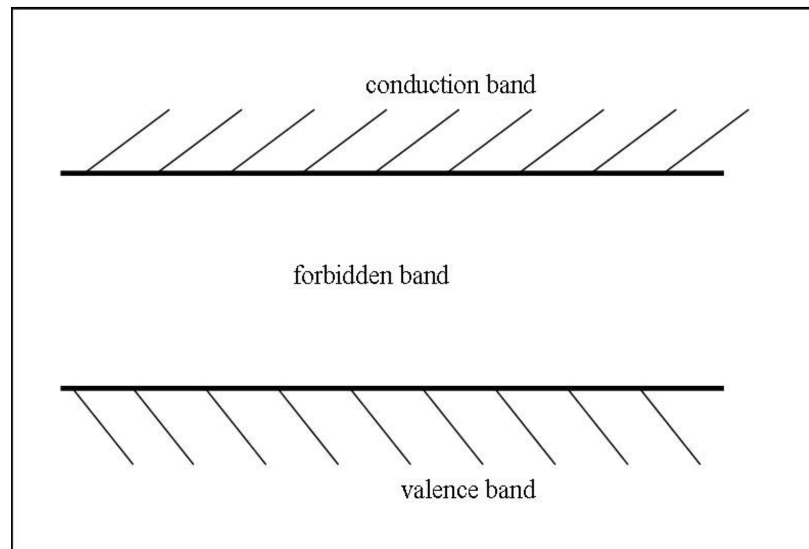

Figure 2.1 Sketch of the conduction, forbidden, and valence bands within a semiconductor

Electrons from the valence band can be readily accelerated into the conduction band at the point or points of intersection of the two bands. So the material can support a current. A semiconductor is like an insulator but with a relatively small energy gap separating the conduction and valence bands. At absolute zero temperature, the conduction band is completely empty and the valence band is completely filled in a semiconductor. However, as the temperature is increased to room temperature, the energy gap is suitably small that some measurable population of the conduction band occurs. Therefore, a semiconductor will conduct a current at room temperature but with a much higher resistance than that of a metal.

Pure elements such as silicon show the importance in many semiconductor devices. In order to change its properties by adding very small but controlled amounts of impurities, it is most often made useful.

II	III	IV	V	VI
	Al	Si	P	S
Zn	Ga	Ge	As	Se
Cd	In	Sn	Sb	Te
Hg				

Figure 2.2 Elements found in elemental and compound semiconductors. Group IV are elemental semiconductors. Compound semiconductors can be formed by combining Groups III and V or II and VI or III and VI

Silicon-based materials command in the semiconductor industry and in electronic devices like computers and calculators. A number of other compounds including GaAs (or gallium arsenide) which is the material used in the laser of a CD player are also used extensively. Some other combinations of elements that exhibit semiconductor properties are indicated on the periodic table above (See Figure 2.2).

As a summary, semiconductor devices now effect our lives on a daily basis. It is known that insulators and conductors are useful in their own right. But semiconductors such as silicon and gallium arsenide have dramatically changed the way in which billions of people live. Their intermediate ability to conduct electricity at room temperature makes them very useful for electronic applications. For instance, the ability of silicon transistors made possible the modern computing industry to act as fast on/off switches.

All materials have energy bands within their electrons can exist. In metals, the valence band is partially-filled and the electrons can move through the material. In semiconductors, however, there is a band gap that exists, and at low temperatures electrons cannot leap the gap easily. Most electrons in semiconductors can jump the energy gap at higher temperatures; and its conductivity increases correspondingly. Electrical properties can also be changed by doping (adding impurities to the semiconductor material).

2.1 Equilibrium Carrier Concentrations and Intrinsic Material

An intrinsic semiconductor also called an undoped semiconductor or i-type semiconductor is a pure semiconductor without any significant dopant species present. The properties of the material determine the number of charge carriers itself instead of the amount of impurities. In intrinsic semiconductors the number of electrons and the number of holes are equal.

Intrinsic semiconductors are essentially pure semiconductor material. The semiconductor material structure should contain no impurity atoms. Elemental and compound semiconductors can be intrinsic semiconductors. At room temperature, the thermal energy of the atoms may allow a small number of the electrons to be involved in the conduction process. Unlike metals, where the resistance of semiconductor material decreases with temperature. For semiconductors, as the temperature increases, the thermal energy of the valence electrons increases, allowing some of them to break through the energy gap into the conduction band.

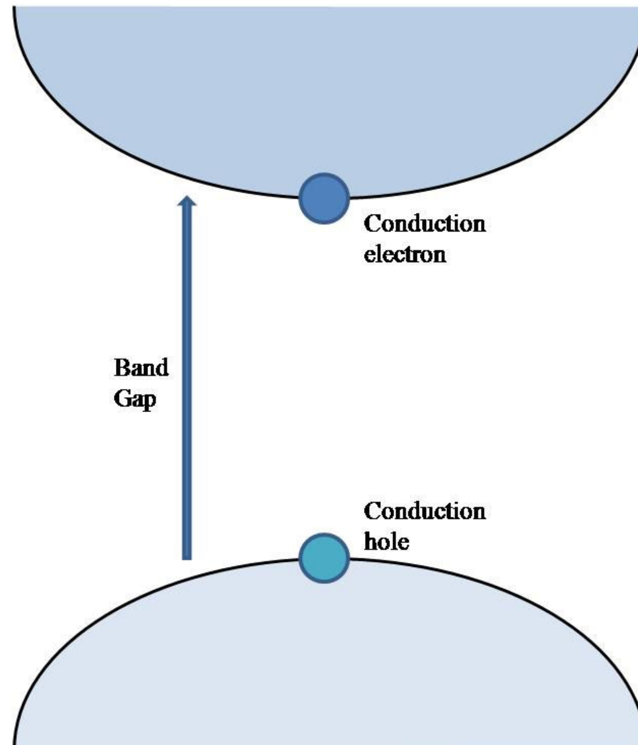

Figure 2.3 Intrinsic semiconductor

When an electron gains enough energy to escape the electrostatic attraction of its parent atom, it leaves behind a vacancy which may be filled by another electron. The vacancy produced can be thought of as a second carrier of positive charge. It is known as a hole. As electrons flow through the semiconductor, holes flow in the opposite direction. If there are n free electrons in an intrinsic semiconductor, then there must also be n holes. Holes and electrons created in this way are known as intrinsic charge carriers. The carrier concentration or charge density explains the number of charge carriers per unit volume. This relationship can be expressed as n=p where n is the number of electrons and p the number of holes per unit volume [90]. The variation in the energy gap between different semiconductor materials means that the intrinsic carrier concentration at a given temperature also changes.

2.2 Extrinsic Semiconductors

An extrinsic semiconductor can be formed from an intrinsic semiconductor by added impurity atoms to the crystal in a process known as doping. By taking as an example Silicon; since Silicon belongs to group IV of the periodic table, it has for valence electrons. In the crystal form, each atom shares an electron with a neighbouring atom. In this state it is an intrinsic semiconductor. B, Al, In, Ga all have three electrons in the valence band [90]. When a small proportion of these atoms, (less than 1 in 10^6), is combined into the crystal the dopant atom has an insufficient number of bonds to share bonds with the surrounding Silicon atoms. One of the Silicon atoms has a vacancy for an electron. It creates a hole that contributes to the conduction process at all temperatures. Dopants that create holes in this manner are known as acceptors. This type of extrinsic semiconductor is known as p-type as it creates positive charge carriers. Elements that belong to group V of the periodic table such as As, P, Sb have an extra electron in the valence band. When added as a dopant to intrinsic Silicon, the dopant atom contributes an additional electron to the crystal. Dopants that add electrons to the crystal are known as donors and the semiconductor material is said to be n-type. Acceptor impurity atoms have less valence electrons than the atoms they replace in the intrinsic semiconductor. They "accept" electrons from the semiconductor's valence band. This provides excess holes to the intrinsic semiconductor. Excess holes increase the hole carrier concentration (p_0) of the semiconductor, creating a p-type semiconductor.

2.2.1 N-type Semiconductors

An N-type semiconductor is obtained by carrying out a process of doping, that is, by adding an impurity of valence-five elements to a valence-four semiconductor in order to increase the number of free (in this case negative) charge carriers.

When the doping material is added, it gives away (donates) weakly-bound outer electrons to the semiconductor atoms. This type of doping factor is also known as donor material since it gives away some of its electrons.

The purpose of n-type doping is to produce an abundance of mobile or "carrier" electrons in the material. To help understand how n-type doping is performed, consider the case of silicon (Si). Si atoms have four valence electrons, each of which is covalently bonded with one of four adjacent Si atoms. If an atom with five valence electrons, such as those from group 15 (old group VA, a.k.a. nitrogen group) of the periodic table (eg. phosphorus (P), arsenic (As), or antimony (Sb)), is combined into the crystal lattice in place of a Si atom, then that atom will have four covalent bonds and one unbonded electron. This extra electron is only weakly bound to the atom and can easily be excited into the conduction band [91].

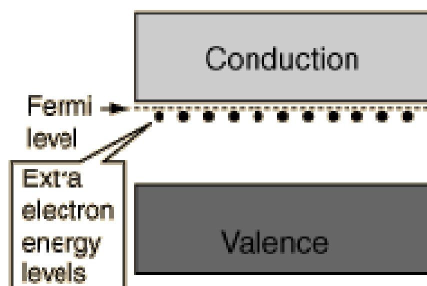

Figure 2.4 N-type semiconductor

At normal temperatures, virtually all such electrons are excited into the conduction band. Since excitation of these electrons does not result in the formation of a hole, the number of electrons in such a material far exceeds the number of holes. In this case the electrons are the majority carriers and the holes are the minority carriers.

Because the five-electron atoms have an extra electron to "donate", they are called donor atoms. Note that each movable electron within the semiconductor is never far from an stationary positive dopant ion, and the N-doped material normally has a net electric charge of zero.

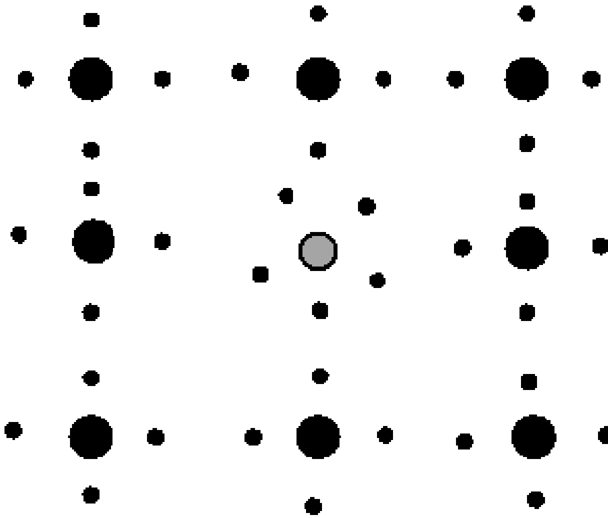

Figure 2.5 N-doped material

2.2.2 P-type Semiconductors

A P-type semiconductor is obtained by carrying out a process of doping, that is adding a certain type of atoms to the semiconductor in order to increase the number of free (in this case positive) charge carriers.

When the doping material is added, it takes away (accepts) weakly-bound outer electrons from the semiconductor atoms. This type of doping factor is also known as acceptor material and the semiconductor atoms that have lost an electron are known as holes.

The purpose of P-type doping is to create an abundance of holes. In the case of silicon, a trivalent atom (typically from group IIIA of the periodic table, such as boron or aluminium) is substituted into the crystal lattice. The result is that one electron is missing from one of the four covalent bonds normal for the silicon lattice. Thus the dopant atom can accept an electron from a neighboring atoms' covalent

bond to complete the fourth bond. Such dopants are called acceptors. The dopant atom accepts an electron, causing the loss of half of one bond from the neighboring atom and resulting in the formation of a "hole". Each hole is associated with a nearby negative-charged dopant ion, and the semiconductor remains electrically neutral as a whole. However, once each hole has wandered away into the lattice, one proton in the atom at the hole's location will be "exposed" and no longer cancelled by an electron. For this reason a hole behaves as a quantity of positive charge. When a sufficiently large number of acceptor atoms are added, the holes greatly outnumber the thermally-excited electrons. Thus, the holes are the majority carriers, while electrons are the minority carriers in P-type materials. Blue diamonds (Type IIb), which contain boron (B) impurities, are an example of a naturally occurring P-type semiconductor.

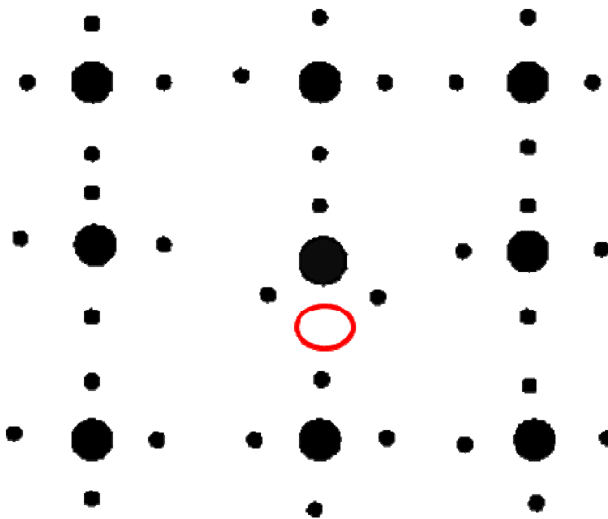

Figure 2.6 P-type semiconductor

The addition of acceptor impurities contributes hole levels low in the semiconductor band gap so that electrons can be easily excited from the valence band into these levels, leaving mobile holes in the valence band. This shifts the effective Fermi level to a point about halfway between the acceptor levels and the valence band.

Electrons can be elevated from the valence band to the holes in the band gap with the energy provided by an applied voltage. Since electrons can be exchanged between

the holes, the holes are said to be mobile. The holes are said to be the "majority carriers" for current flow in a p-type semiconductor.

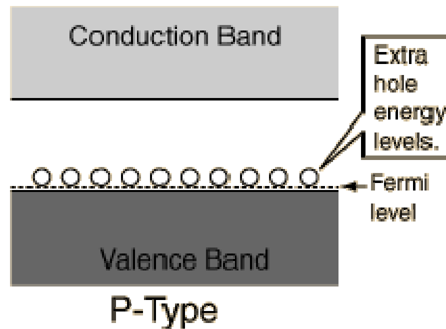

Figure 2.7 P-type material's energy bands

2.3 Band Gap of Semiconductors

In solid state physics and related applied fields, the band gap, also called an energy gap or stop band, is a region where a particle or quasiparticle is forbidden from propagating. For insulators and semiconductors, the band gap generally refers to the energy difference between the top of the valence band and the bottom of the conduction band.

In semiconductors and insulators, electrons are confined to a number of bands of energy, and forbidden from other regions. The term "band gap" refers to the energy difference between the top of the valence band and the bottom of the conduction band, where electrons are able to jump from one band to another.

The conductivity of intrinsic semiconductors is strongly dependent on the band gap. The only available carriers for conduction are the electrons which have enough thermal energy to be excited across the band gap.

The distinction between semiconductors and insulators is a matter of convention. One approach is to consider semiconductors a type of insulator with a low band gap. Insulators with a higher band gap, usually greater than 3 eV, are not considered semiconductors and generally do not exhibit semiconductive behaviour under practical conditions.

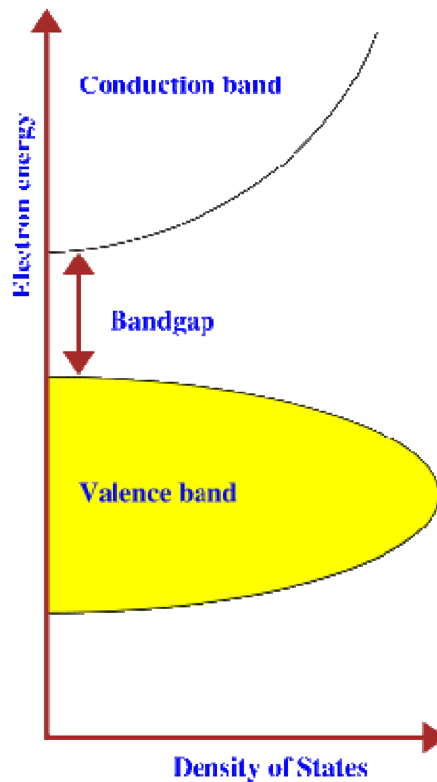

Figure 2.8 Band gap diagram of semiconductor

2.3.1 Direct Gap Transition

In semiconductor physics, a direct bandgap means that the minimum of the conduction band lies directly above the maximum of the valence band in momentum space.

In a direct bandgap semiconductor, electrons at the conduction-band minimum can combine directly with holes at the valence band maximum, while conserving momentum. The energy of the recombination across the bandgap will be emitted in the form of a photon of light. This is radiative recombination, also called spontaneous emission [92].

A photon (a "particle of light") with energy $E = \hbar\omega$ can be absorbed by promoting a valence band electron to the conduction band, creating an electron-hole pair.

This is a two body collision (electron, photon).

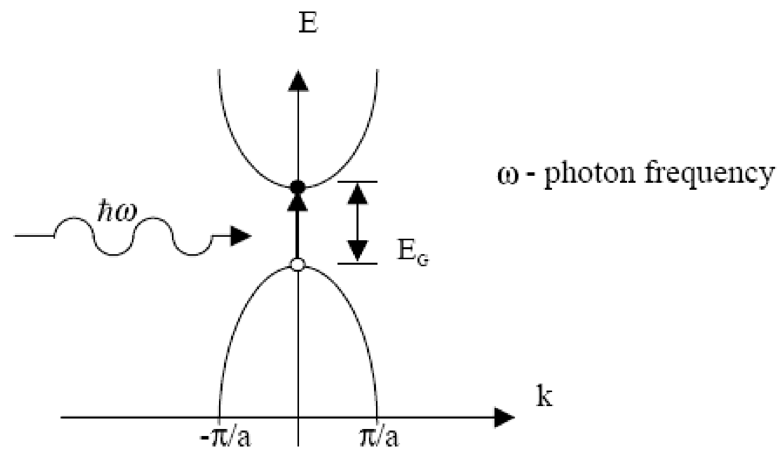

Figure 2.9 (Δk = 0) Change of electron momentum is zero

2.3.2 Indirect Gap Transition

In indirect bandgap semiconductors such as crystalline silicon, the momentum of the conduction band minimum and valence band maximum are not the same, so a direct transition across the bandgap does not conserve momentum and is forbidden. Recombination occurs with the mediation of a third body, such as a phonon or a crystallographic defect, which allows for conservation of momentum. These recombinations will often release the bandgap energy as phonons, instead of photons, and thus do not emit light. As such, light emission from indirect semiconductors is very inefficient and weak.

Semiconductors that have an indirect band gap are inefficient at emitting light. This is because any electrons present in the conduction band quickly settle into the energy minimum of that band. Electrons in this minimum require some source of momentum allowing them to overcome the offset and fall into the valence band. Photons have very little momentum compared to this energy offset. The momentum "kick" of a photon being emitted or absorbed is negligible and direct transitions are essentially vertical in k-space.

Since the electron cannot rejoin the valence band by radiative recombination, conduction band electrons typically last quite some time before recombining through

less efficient means. Silicon is an indirect band gap semiconductor, and hence is not generally useful for light emitting diodes or laser diodes.

Likewise the absorption of light at an indirect gap is much weaker than at a direct one. As in the emission process both the laws of conservation of energy and momentum must be observed, the only way to promote electron from the top of the valence band to the bottom of the conduction band is to simultaneously emit (or absorb) a phonon that compensates for the missing momentum vector [92]. However, such a combined transition has a much probability.

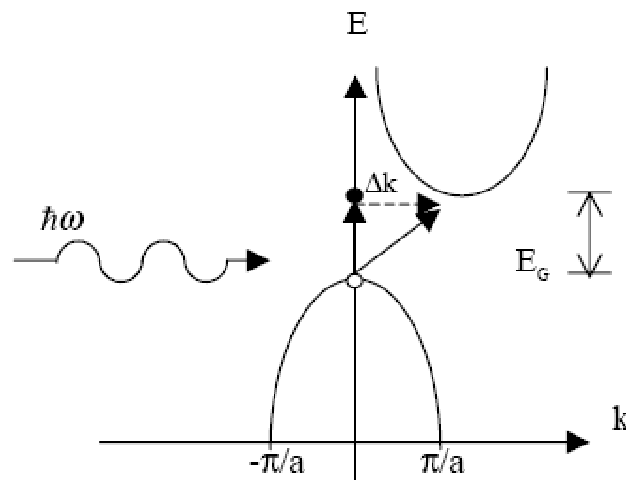

Figure 2.10 ($\Delta k \neq 0$) Change of electron momentum is non zero

A photon carries little momentum, for a transition we need Δk (a momentum change) and this can not be provided by the photon itself.

Promotion of valence band electron to conduction band requires momentum transfer from crystal lattice (interaction with a “phonon”); this is a relatively unlikely event as it is a three body collision (electron, photon, phonon).

“phonon” = quantized lattice vibration (“particle” of heat)

Light absorption is relatively weak.

Note: all semiconductors are effectively - transparent for light with $h\nu < E_G$ (no possible transition).

- absorb for $h\nu > E_G$ (transitions allowed)

2.4 Absorption in Semiconductors

Light normally incident on a solid will be partially reflected at the air (or vacuum) and solid interface, and the remaining light will enter the solid. If it is absorbed by the solid, its intensity will decrease exponentially with distance as $e^{-\alpha(\lambda)x}$, where $\alpha(\lambda)$ is the absorption coefficient.

$$I(\lambda,x) = I_0(\lambda)\, e^{-\alpha(\lambda)x} \qquad (1.1)$$

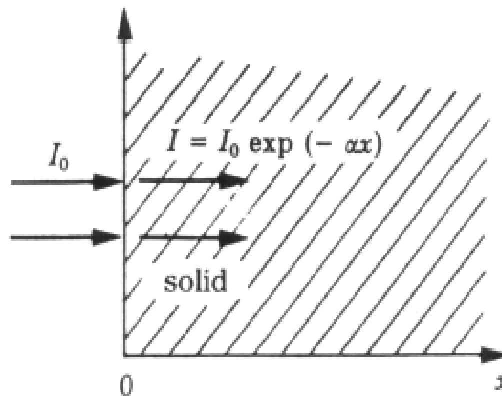

Figure 2.11 Model for light absorption

Within these energy level systems we can have a variety of mechanisms by which electrons (and holes) absorb optical energy. Most of these processes can occur in quantum wells, wires, and dots, as well as in bulk material [93]:

Band-to-band: an electron in the valence band absorbs a photon with enough energy to be excited to the conduction band, leaving a hole behind.

Band-to-exciton: an electron in the valence band absorbs almost enough energy to be excited to the conduction band. The electron and hole it leaves behind remain electrically "bound" together, much like the electron and proton of a hydrogen atom.

Band-to-impurity or impurity to band: an electron absorbs a photon that excites it from the valence band to an empty impurity atom, or from an occupied impurity atom to the conduction band.

Free carrier: an electron in the conduction band, or hole in the valence band, absorbs a photon and is excited to a higher energy level within the same set of bands (i.e, conduction or valence).

2.5 Band Theory of Solids and Semiconductors

The energy levels are so closely spaced that they form bands since the very large number of atoms interact in a solid material. The highest energy filled band, which is similar to the highest occupied molecular orbital in a molecule (HOMO), is called the valence band. The next higher band, which is similar to the lowest unoccupied molecular orbital (LUMO) in a molecule, is called the conduction band. The energy separation between these bands is said to be the energy gap, E_g.

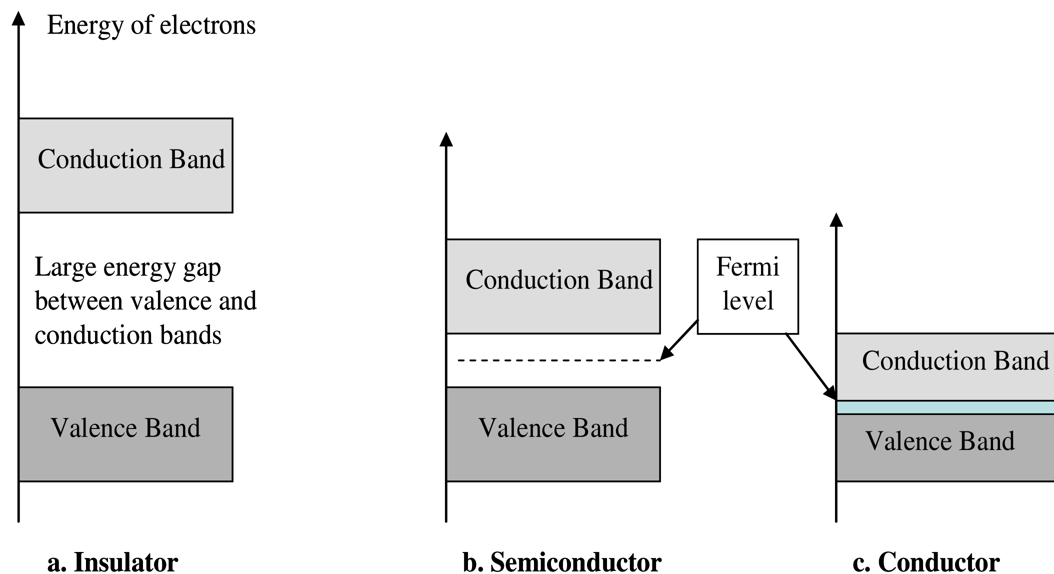

Figure 2.12 Band diagrams for insulator, semiconductor, and conductor

The filling of these bands and the size of the energy gap determine if a material is a conductor (a metal), a semiconductor, or an insulator. In metals there is no energy

gap between filled and unfilled energy levels. An important number of electrons are thermally excited into empty levels, creating holes in the filled band. The electrons in a conduction band and the holes in a valence band can move throughout the material, allowing it to easily conduct electricity. In semiconductors E_g is small, but large enough so that a fairly small number of electrons are in the conduction band due to thermal energy, and these materials conduct poorly. In insulators E_g is large so that electrons are not promoted to the conduction band due to thermal energy, and these materials do not conduct electricity.

Semiconductors are insulators with a smaller energy gap. Intrinsic semiconductors (not doped by another element) conduct caused by the effect that increasing the temperature will raise the energy of some electrons to reach the conduction band. Since at absolute zero temperature the valence band of semiconductors is completely filled and the conduction band is completely empty, the Fermi energy is in the middle of the bandgap. The fermi distribution is not anymore rectangular, box-shaped at increasing temperature, but rather goes smoothly from 1 to zero as one increases the energy [94]. It will be smaller than one near the top of the valence band and nonzero at the bottom of the conduction band. This means that the conduction band is not filled any more, some electrons are missing from it. These missing electrons are called holes. The same number of electrons appear in the conduction band.

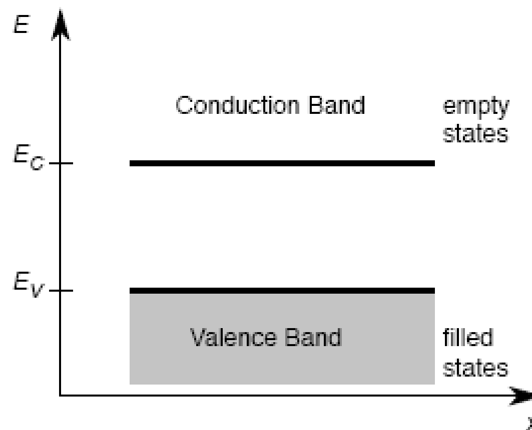

Figure 2.13 Band diagram for a semiconductor, plotting E versus x

In other words, electron-hole pairs are created by thermal excitations. Holes can hop from state to state inside valence band so they also act as charge carriers. Being positive they move under the influence of external fields, contribute to electric conduction.

Light absorption, with photon energy $h\upsilon \geq E_g$, can be described as a valence band electron making a transition to a conduction band state. Light with photon energy $h\upsilon \leq E_g$ is not absorbed and passes through the material.

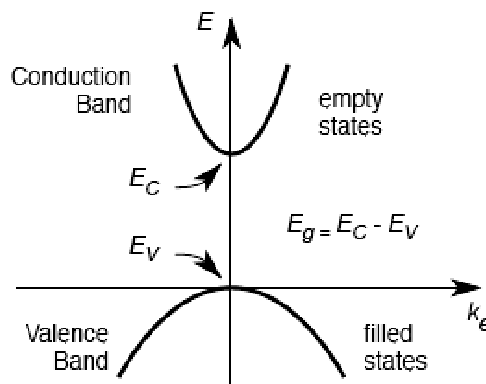

Figure 2.14 Dispersion diagram near the band edges

2.6 Compound Semiconductors

Compound semiconductors which consist of various elements have widely ranging physical properties. They have many possible applications. The physical properties which may vary, include bandgaps, crystal lattice structures, electron and hole mobilities, optical properties, thermal conductivity, and so on. By selecting suitable compound semiconductor materials, it becomes possible to understand various devices which can not be succeeded using the main elemental semiconductor material, silicon. It is therefore important to realize the physical properties of compound semiconductors and to know how to select appropriate materials for desired applications.

Compound semiconductors formed from III–VI elements are key materials in plans to harvest energy directly from sunlight in photovoltaic devices. These are the recent advances in thin film deposition and nanocrystallite synthesis. Current work has significant potential for low-cost, scalable solar cells [95].

Among many compounds which are composed of more than two elements, some show semiconductor properties. Compounds which show semiconductor properties have the following features according to Wilson's model.

(i) The conductivity of the semiconductor is electronic. Ionic conductivity is excluded.
(ii) Conductivity is largely increased as a function of temperature.
(iii) Conductivity is very dependent on the kind of impurities and their concentrations.

Table 2.1 Compound semiconductors

	Variations of Compound Semiconductors
Elemental	Si,Ge
II-VI compound	CdS,CdSe,CdTe,ZnS,ZnSe,ZnTe
III-V compound	GaP,GaAs,GaSb,InP,InAs,InSb
IV-VI compound	PbS,PbSe,PbTe
IV-IV compound	SiC
V-VI compound	Bi_2Te_3
III-VI compound	AlN,GaN,InN,AlP,AlAs,InSe,InS

Compound semiconductor materials can be predicted by a simple rule. When the total number of valence electrons of constituent elements are divided by the number of elements including the compound and when this ratio gives four, the compound has a tendency to be semiconducting.

	I A	II A	III A	IV A	V A	VI A
2					N	
3			Al	Si	P	S
4	Cu	Zn	Ga	Ge	As	Se
5	Ag	Cd	In	Sn	Sb	Te
6	Au	Hg				

III-V

II-VI

I-III-VI_2

Figure 2.15 Periodic table for compound semiconductors

Materials which show semiconducting properties have to obey the following laws.

(i) Regarding elemental semiconductors, the constituent atom has eight electrons including electrons which form covalent bonds and these electrons produce ***s,*** p orbital closed shells.

(ii) For compound semiconductors, the condition (i) is applied to each constituent atom.

Elements from IV group to VII group satisfy the first condition (i) and following the second condition (ii), compound semiconductors include these elements.

2.6.1 III-VI Family Compound Semiconductors

III-VI compound semiconductors are interesting because of their potential applications in the field of optoelectronics. These materials have a layered structure, where the bonds within the layers are mainly covalent and layers are bounded by van der Waals forces. Identifying with the bound anisotropy interesting distinctive properties appear, which have been the object of an excessive research work.

An analysis is made of the many theoretical and experimental studies of layered crystals. The results of this analysis for the particular case of group III-VI semiconductors are used to inspect the features in the electronic and phonon spectra in order to reveal structural anisotropy of these compounds [96].

III-VI compound semiconductors include: AlN, GaN, InN, AlP, AlAs, AlSb, GaP, GaAs, GaSb, InP, InAs, InSb, $Al_xGa_{1-x}As$ and $In_xGa_{1-x}As$. In the family of III-VI semiconductors, GaS, GaSe, and InSe have been the more studied compounds.

2.6.1.1 In_2S_3 Semiconductors

In_2S_3 is a member of III-VI semiconductor group including GaS, GaSe and InSe layered crystals. The crystal structure of In_2S_3 could be considered as a three-dimensional network somewhat different from the layered structure of its counterparts. The III-VI compounds recently attracted attention due to their semiconducting nature and applications in radiation detectors, optoelectronic devices, and electrical switching. Literature concerning the preparation and physical properties of In_2S_3 crystal is relatively unusual on account of the difficulty of growing large single crystals.

In_2S_3 films are promising candidates for many technological applications due to their air stability, their transparency, their band gap energy and their photoconductor behaviour. In_2S_3, III–VI group material, crystallizes in four polymorphic phases, namely α, cubic β, tetragonal γ and ε, as function of temperature and preparation conditions. It has been the most widely studied semiconductor compound in the In-S system. It is known to be an n-type semiconductor with a direct band gap and can be used as a buffer layer of heterojunction solar cells. It is well known that structural and morphological properties of deposited thin films are strongly influenced by deposition conditions [97]. For this reason, the knowledge of this influence could help researchers to select appropriate conditions for obtaining films with suitable characteristics semiconductor technology.

In recent times, β-In_2S_3 thin films has attaracted attention. It is a significant material for opto-electronic and photovoltaic applications, and a promising candidate for

many technological applications due to its stability, its interesting structural characteristics, and also its optical, acoustical and electronical properties. Furthermore, it takes the place of CdS buffer layers for environmental reasons by using a material with a wider bandgap compared to CdS [98]. Among others, indium sulphide has been acknowledged as a satisfactory alternative material.

Indium sulphide is a chalcogenide semiconductor useful in the preparation of green and red phosphors, for the manufacture of picture tubes for colour televisions and dry cells. It has indicated excellent results on small areas. Recently, highly supporting results have been reported for indium sulphide prepared by thermal evaporation, modulated flux deposition, chemical bath deposition and by rietveld method [97].

2.7 Crystal Structure

2.7.1 Unit Cell

The crystal structure of a material is often discussed in terms of its unit cell. The unit cell is a spatial arrangement of atoms which is tiled in three-dimensional space to describe the crystal. The unit cell is given by its lattice parameters, the length of the cell edges and the angles between them, while the positions of the atoms inside the unit cell are described by the set of atomic positions (x_i,y_i,z_i) measured from a lattice point.

For each crystal structure there is a conventional unit cell, which is the smallest unit that has the full symmetry of the crystal. However, the conventional unit cell is not always the smallest possible choice.

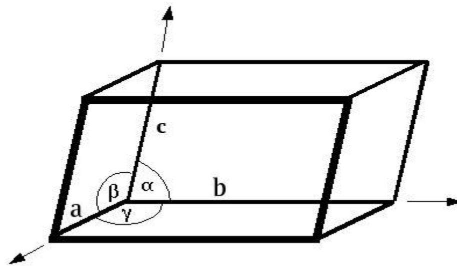

Figure 2.16 Unit cell

A primitive unit cell of a particular crystal structure is the smallest possible unit cell one can construct such that, when tiled, it completely fills space. This primitive unit cell does not, however, display all the symmetries inherent in the crystal.

There are only seven possible crystal systems that atoms can pack together to produce an infinite 3D space lattice in such a way that each lattice points has an identical environment to that around every other lattice point.

2.7.2 Crystal Lattice

A crystal is a regular, ordered arrangement of atoms over a large scale. The atoms may be of a single type or the repetition of a complex arrangement of many different types of atoms. The crystal can be thought of as consisting of two separate parts: the lattice and the basis. The lattice is an ordered arrangement of points in space, while the basis consists of the simplest arrangement of atoms which is repeated at every point in the lattice to build up the crystal structure.

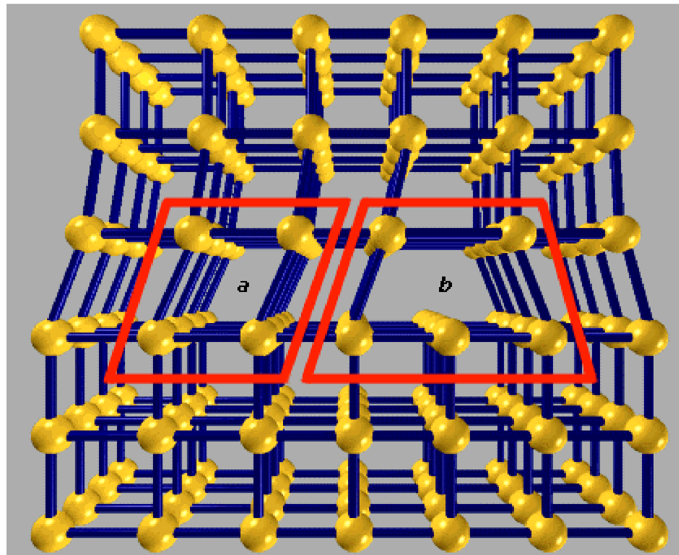

Figure 2.17 Crystal lattice

Most solids have periodic arrays of atoms which form what we call a crystal lattice. Amorphous solids and glasses are exceptions. The existence of the crystal lattice implies a degree of symmetry in the arrangement of the lattice, and the existing

symmetries have been studied extensively. One of the implications of the symmetric lattice of atoms is that it can support resonant lattice vibration modes. These vibrations transport energy and are important in the thermal conductivity of non-metals, and in the heat capacity of all solids.

2.7.3 Crystal System

The crystal systems are a grouping of crystal structures according to the axial system used to describe their lattice. Each crystal system consists of a set of three axes in a particular geometrical arrangement. There are seven unique crystal systems. The simplest and most symmetric, the cubic (or isometric) system, has the symmetry of a cube.

When the crystal systems are combined with the various possible lattice centerings, it is arrived at the Bravais lattices. They describe the geometric arrangement of the lattice points, and thereby the translational symmetry of the crystal. In three dimensions, there are 14 unique Bravais lattices which are distinct from one another in the translational symmetry they contain. The fourteen three-dimensional lattices, classified by crystal system.

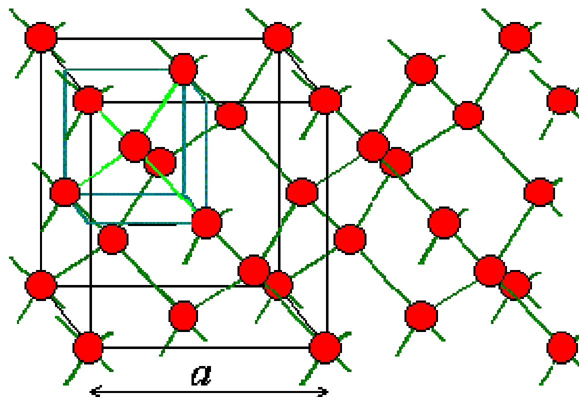

Figure 2.18 Crystal system

The crystal structure consists of the same group of atoms, the basis, positioned around each and every lattice point. This group of atoms therefore repeats

indefinitely in three dimensions according to the arrangement of one of the 14 Bravais lattices.

2.7.4 Semiconductor Crystal

Most solids have periodic arrays of atoms which form what we call a crystal lattice. The existence of the crystal lattice implies a degree of symmetry in the arrangement of the lattice, and the existing symmetries have been studied extensively.

Solid materials are classified by the way the atoms are arranged within the solid. Materials in which atoms are placed at random are called amorphous. Materials in which atoms are placed in a high ordered structure are called crystalline. Poly-crystalline materials are materials with a high degree of short-range order and no long-range order. These materials consist of small crystalline regions with random orientation called grains, separated by grain boundaries.

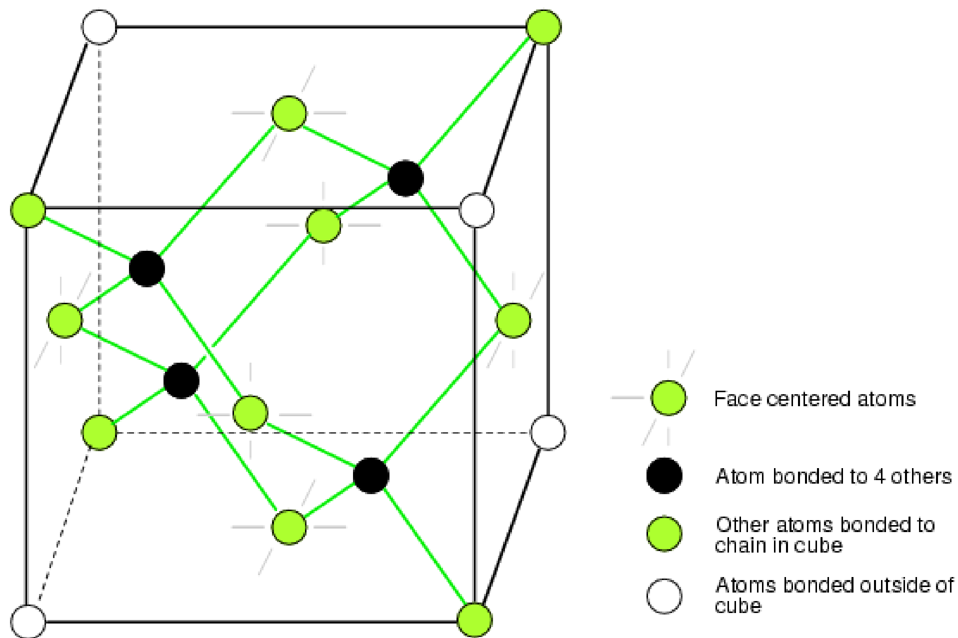

Figure 2.19 Semiconductor crystal

In Fig. 2.19 shows four atoms (dark) bonded to four others within the volume of the cell. This is equivalent to placing at the origin in Fig. 2.19, then placing three more

on adjacent faces to fill the full cube. Six atoms fall on the middle of each of the six cube faces, showing two bonds. The other two bonds to adjacent cubes were omitted for clarity. Out of eight cube corners, four atoms bond to an atom within the cube. The other four bond to adjacent cubes of the crystal. Although four corner atoms show no bonds in the cube, all atoms within the crystal are bonded in one giant molecule. A semiconductor crystal is built up from copies of this unit cell [99].

Of primary interest are crystalline semiconductors in which atoms are placed in a highly ordered structure. Crystals are categorized by their crystal structure and the underlying lattice. While some crystals have a single atom placed at each lattice point, most crystals have a combination of atoms associated with each lattice point. This combination of atoms is also called the basis.

CHAPTER 3

EXPERIMENTAL STUDIES

3. THIN FILM PRODUCTION TECHNIQUES

3.1 Spray Pyrolysis Method

3.1.1 Introduction

The spray pyrolysis technique (or solution spraying) for the growth of semiconducting films is a method of spraying a suitable solution mixture onto a heated substrate. It is a convenient and economical method for the deposition of such materials. This technique simply consists of spraying a finely atomised solution onto a suitable hot substrate. The substrate temperature has a greate influence on the spraying of the films. The spray nozzle strongly affects the spraying rate, the sprayed particle size and the spray distribution. In the spray pyrolysis process the uniformity of the droplet size is one of the primary requirements for a spray system. The chemicals contained in the spray solution are expected to fullfil the following conditions;

(i)- The chemicals in the spray solution provide species/complexes that will undergo a thermally activated chemical reaction to yield the desired film material,

(ii)- The remainder of the constituents including the carrier liquid should be volatile at the substrate temperature.

3.1.2 Experimental Set-up of Spraying System

In this study, the apparatus which is used for the development of film samples based on the spraying pyrolysis technique has been designed and developed in our laboratory. A schematic block diagram of an experimental apparatus used for spray pyrolysis is shown in Fig. 3.1. This system consists of a spraying system, heater, temperature control system, and timer. The system is enclosed by a glass chamber.

3.1.3 Deposition Apparatus

In this thesis, the apparatus which we used for the development of the thin film samples is based on the spraying pyrolysis technique. This apparatus whose schematic diagram is given in Fig. 3.1 consists of a spraying system, heater, temperature control system and timer.

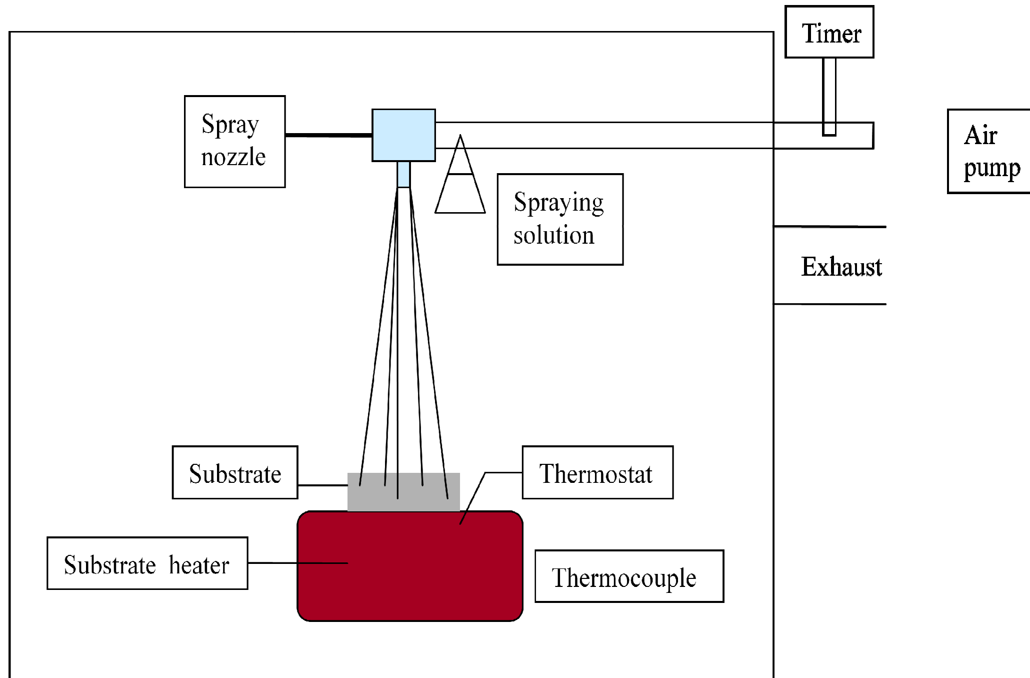

Figure 3.1 Schematic diagram of the spray pyrolysis system

Spraying system: This is used to produce the bubbles from the spraying solution. The bubbles can be in different sizes depending on the geometry of the nozzle, as seen in Fig. 3.1 above, being employed to produce the bubbles and also the flow rate of the carrier gas. In this study, air is used as carrier gas and the flow rate of the spraying solution is regulated by air.

Heater: This is used to heat the substrates. It is consisted of a steel plate with a resistance coil lying under it. The power of the heater is 2500 watts and it operates at 220 volts and 50 Hz (AC).

Temperature control system: A thermostat is used to keep the substrates at required temperatures. One of the most important factors which plays a vital role for producing high quality film samples is to keep the substrates at required temperatures. The substrate temperature is controlled to within an accuracy of $\pm 5^0$C by thermostat system.

Glass chamber: The spraying system and the heater are placed in a glass chamber and nitrogen gas is passed through during the growth of the thin film.

3.2 Growth Mechanism of The Semiconducting Films by The Spraying Pyrolysis Method

3.2.1 Introduction

The spray pyrolysis technique for the production of semiconducting films is a method of spraying suitable solution mixtures onto a heated substrate. This method is convenient and economical method for the deposition of such materials. Several factors influence the proper performance and the quality of semiconducting film produced by the spraying pyrolysis method. These factors are as follows: (i) the properties of substrate, (ii) the substrate temperature, (iii) the spray nozzle, (iv) the uniformity of the droplet size of solution, (v) the flow rate of spraying solution, and (vi) the height of the nozzle from the substrate surface.

3.2.2 Substrate Preparation

The physical properties of substrates on which films are deposited, play a vital role in the growth of good quality film samlpes. The film properties are very strongly dependent on the crystal structure of substrate. The crystalline films can be deposited on a noncrystalline material such as glass, ceramic and mica. In this study, glass is used as substrate because of its cheepness when compared to other types of substrate. The preparation of glass substrate is as follows. Firstly, the glass substrates are cut into 0.5 cm^2 in size. A cleaning process of the glass substrate is carried out in four steps as seen in Fig. 3.2.

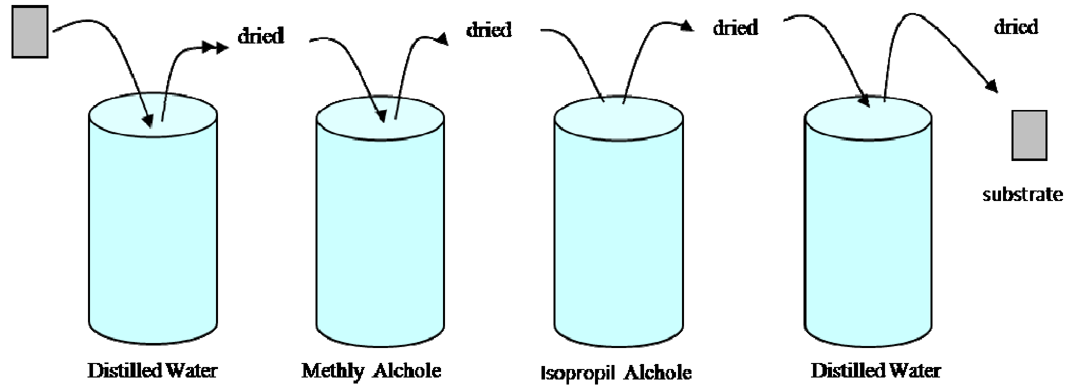

Figure 3.2 Cleaning process of the glass substrate

The cleaning process is as follows:

1- The glass substrate is immersed into the distilled water to clean the dust on its surface for 15 minutes. Then it is taken out from the distilled water and dried.

2- The substrate which is taken from the first cup and dried, is immersed into the methyl alcohol and left there for 15 minutes to clean the oil substance on the surface of the substrate, and then it is taken out from this liquid and dried in air.

3- The dried substrate is immersed into the third cup filled with isopropil alcohol and it is treated again for 15 minutes to obtain a smooth surface.

4- Finally, the substrate is treated with the distilled water as in the first step to clean all the residues remaining on the surface of substrate during the other processes.

3.2.3 Spraying Solution Preparation

The spraying solution is prepared for the production of In_2S_3 film as follow; firstly, the required amounts of indium chloride ($InCl_3$) and thiourea $CS(NH_2)_2$ salts are weighted by high sensible electronic balance and stirred together into a cup containing the distilled water of 100 mlt to form the solution. Different spraying solutions were used for the production of semiconducting In_2S_3 films with different compositions.

3.2.4 Development of In_2S_3 Films

Spray pyrolysis involves in the application of a fine mist of very small droplets containing the reactants onto the hot substrates. During the deposition process, the precursor solution is pulverized onto the substrates. The droplets undergo evaporation, solute condensation, and thermal decomposition, which then result into the film formation.

In_2S_3 films were obtained on the glass substrates by spray pyrolysis method. The initial solution was prepared from indium chloride ($InCl_3$) at 0.5 M concentration and 0.5 M thiourea $CS(NH_2)_2$ in deionized water. The substrate temperature was varied in the range of 330-380 ^oC. The solution and carrier gas flow rates were 5 cm^3 min^{-1} and 5 dm^3 min^{-1}, in all cases. Air was used to atomize the spray. Consistent conditions of substrate temperature and flow rate of carrier gas were maintained during deposition of such films. The formation of In_2S_3 resulted from the chemical reaction is

$$2InCI_3 + 3CS(NH_2)_2 + 6H_2O \rightarrow In_2S_3 + 3CO_2 + 6NH_4CI$$

As seen the above equation, after solution was mixed with indium chloride ($InCI_3$) and thiourea ($CS(NH_2)_2$) , In_2S_3 film was formed as a solid on the glass substrate and CO_2 was thrown as a gas. And also NH_4CI is given out as a vapor.

CHAPTER 4

4. MEASUREMENT METHODS

4.1 Compositional Analysis

This analysis was carried out by EDX Analysis stands for Energy Dispersive X-ray analysis. It is a technique used for identifying the elemental composition of the specimen, or an area of interest thereof. This technique is used in conjunction with SEM and is not a surface science technique. An electron beam strikes the surface of a conducting sample. The energy of the beam is typically in the range 10-20keV. This causes X-rays to be emitted from the point in the material. The energy of the X-rays emitted depend on the material under examination.

During EDX Analysis, the specimen is bombarded with an electron beam inside the scanning electron microscope. The bombarding electrons collide with the specimen atoms' own electrons, knocking some of them off in the process. A position vacated by an ejected inner shell electron is eventually occupied by a higher-energy electron from an outer shell. To be able to do so, however, the transferring outer electron must give up some of its energy by emitting an X-ray [100].

The output of an EDX analysis is an EDX spectrum. The EDX spectrum is just a plot of how frequently an X-ray is received for each energy level. An EDX spectrum normally displays peaks corresponding to the energy levels for which the most X-rays had been received. Each of these peaks are unique to an atom, and therefore corresponds to a single element. The higher a peak in a spectrum, the more concentrated the element is in the specimen.

The x-axis of the spectrum is the X-ray energy scale, along which X-rays collected from various elements are registered, and which in turn form a series of peaks along the x-axis where each peak corresponds to a particular element. With modern software, it is possible to collect a series of spectrums for each point (pixel) analysed by the electron beam probe, as it is scanned across the surface of the specimen. If one

spot only is analysed, quantification of the relative proportions of elements under that spot is possible, which is known as point analysis. If however a line of pixels is analysed, a line-traverse analysis can be performed which can highlight changing proportions of elements with distance along the line. This is known as line scanning. Finally, each pixel in an image can also be analysed, which illustrates the distribution of a chosen element across the image. This is known as dot-mapping of the elements, and can take up some considerable time as the electron probe is required to dwell on each separate point for a pre-determined period of time in order to collect enough data for analysis.

4.2 X-ray Studies

Structural properties of the deposited films were studied by X-ray diffraction (XRD) technique. The X-ray measurements were performed using CuK_α radiation (λ=1.542Å) from a conventional θ - 2θ diffractometer (D 5000 Siemens). The peaks (2θ) of the XRD patterns of the film samples were identified by using Bragg diffraction law equation as given below.
The lattice constant 'a' for the cubic phase structure is determined by the relation

$$a^2 = \frac{\lambda^2 (h^2 + k^2 + l^2)}{4\sin^2\theta} \quad (4.1)$$

where θ is the diffraction spectra (Bragg's angle), λ is the wavelength of the X-ray. The line profiles were measured by means of point by point cutting using a fix period 20s and 2θ increment of 0.02^o.

From the XRD profiles, the inter-planar spacing d_{hkl} was calculated for the (220) plane using the Bragg's relation [102]

$$d_{hkl} = \frac{n\lambda}{2\sin\theta} \quad (4.2)$$

where λ is the wavelength of the X-ray used, d is the lattice spacing, n is the order number and θ is the Bragg's angle. The factor d is related to (h k l) indices of the

planes and the dimension of the unit cells. The crystallite size (D) of the films was calculated from the Debye Scherrer's formula from the full-width at half-maximum (FWHM) β of the peaks expressed in radians [109]

$$D = \frac{0.94\lambda}{\beta \cos\theta} \tag{4.3}$$

where β is the FWHM calculated from the (220) plane. The strain value (ε) can be evaluated by using the following relation

$$\beta = \frac{\lambda}{D\cos\theta} - \varepsilon \tan\theta \tag{4.4}$$

The dislocation density (δ), defined as the length of dislocation lines per unit volume of the crystal and has been calculated by using the formula [109]

$$\delta = \frac{1}{D^2} \tag{4.5}$$

The lattice parameter 'a' can be calculated from the equation given below for cubic geometry.

$$\frac{1}{d^2} = \frac{(h^2 + k^2 + l^2)}{a^2} \tag{4.6}$$

where h, k, l represent the lattice planes. The values of particle size, strain and dislocation density for the films of different substrate temperatures are calculated by using the above equations(Eq.(4.3),(4.4),(4.5),(4.6)).

4.3 Optical Characterization

An important technique used for the determination of the band gap energy of a semiconductor is the absorption of incident photons by material. Optical absorption studies of the sprayed In_2S_3 films on the glass substrate have been carried out in the

wavelength range of 300 nm to 900nm employing a UV/VIS spectrophotometer (Jasco 7800 model). To determine the energy band gap values of the samples, it is necessary to determine the value of the absorption coefficients of the samples corresponding to different wavelengths of the photons. For this purpose, a Jasco 7800 Model Spectrometer was used for the transmission and absorption measurements. The absorption coefficient of sample corresponding to different wavelengths can be calculated from following equation:

$$\frac{I}{I_0}(transmission) = e^{-\alpha t} \tag{4.7}$$

where t is the thickness of the film sample, $T=I/I_0$ is the transmittance (I_0 is the incident light intensity and I is the transmitted light intensity).

By using α values, the optical band gap of the film sample can be determined by means of the following equation:

$$\alpha = \frac{A}{h\nu}(h\nu - E_g)^{1/2} \tag{4.8}$$

where A is a constant, E_g is the energy band gap of film, h is the Planck constant, $\nu=c/\lambda$, c is the speed of light and λ is the wavelenght of light.

4.4 SEM Analysis

The SEM instrument has many applications across different industry sectors. The extremely high magnification images together with localised chemical information enables the instrument to solve a great deal of common industrial issues such as **particle analysis**, defect identification materials and metallurgical problems. An SEM is essentially a high magnification microscope, which uses a focused scanned electron beam to produce images of the sample with the necessary sample preparation, cross-sections.

SEM creates different images by focusing a high energy beam of electrons onto the surface of a sample end detecting signals from the interaction of the incident

electrons with the sample's surface. The types of signals collected in a SEM alters and can comprise secondary electrons, characteristic X-rays, and back scattered electrons. In a SEM, these signals come not only from the primary beam infringing on the sample, but from other interactions within the sample near the surface. The SEM is capable of producing high resolution images of a sample surface in its primary use mode, secondary electron imaging. Due to the manner in which this image is created, SEM images have great depth of field yielding a characteristic three-dimensional appearance useful for understanding the surface structure of a sample. This great depth of field and the wide range of magnifications are the most familiar imaging mode for specimens in the SEM [101]. Characteristic X-rays are emitted when the primary beam causes the ejection of inner shell electrons from the sample and are used to tell the elemental composition of the sample. The back-scattered electrons emitted from the sample may be used alone to form an image or in conjunction with the characteristics X-rays as atomic number contrast clues to the elemental composition of the sample.

A SEM may be equipped with an EDX analysis system to enable it to perform compositional analysis on specimens. EDX analysis is useful in identifying materials and contaminants, as well as estimating their relative concentrations on the surface of the specimen.

CHAPTER 5

5. RESULTS AND DISCUSSION

5.1 Effect of The Substrate Temperature on The Film Formation

The depositions were carried out at substrate temperatures between 200 and 350 ºC using 0.5 M solution. It is observed that the lower substrate temperatures (<250 ºC) result into a non-uniform and easily detachable film formation. The temperature may be insufficient in this case, to decompose the sprayed droplets of the mixed solution. At higher substrate temperatures (>350 ºC), also non-uniform and easily detachable films result. This may be due to higher rates of evaporation of initial ingredients from the surface of the hot substrates. However, the films prepared at intermediate substrate temperatures are uniform and good adherent to the glass substrates.

5.2 Compositional Analysis

The compositional analysis of the films was carried out using energy dispersive X-ray analysis technique, JOEL-JSM-5600, (EDX) to study the Stoichiometry of the films. Fig. 5.1 shows the energy dispersive analysis by X-ray spectrum for In_2S_3 films on the glass substrate by spray pyrolysis method. The films obtained by spray pyrolysis from the spray solution with concentration of 0,5 M indium chloride ($InCl_3$) and 0,5 M thiourea ($CS(NH_2)_2$) were deposited at a substrate temperature of 350 ºC. The EDX results taken from a dark area on the film show that the film contains small amounts of O, Na, and Si; these elements are due to the elemental characteristics of the glass substrate. Carbon and Cl element are due to the $CS(NH_2)_2$ and $InCl_3$ solutions which were used as a source of sulphur and indium for the In_2S_3 film, respectively.

And it is also possibility that oxygen may be incorporated into the film either from the atmosphere or from the deionized water solution. EDX results show that a In_2S_3 film was formed. Analytical results of EDX show that the atomic percent of In (indium) to S (sulphur) on the film was 55.61:44.39(at%)

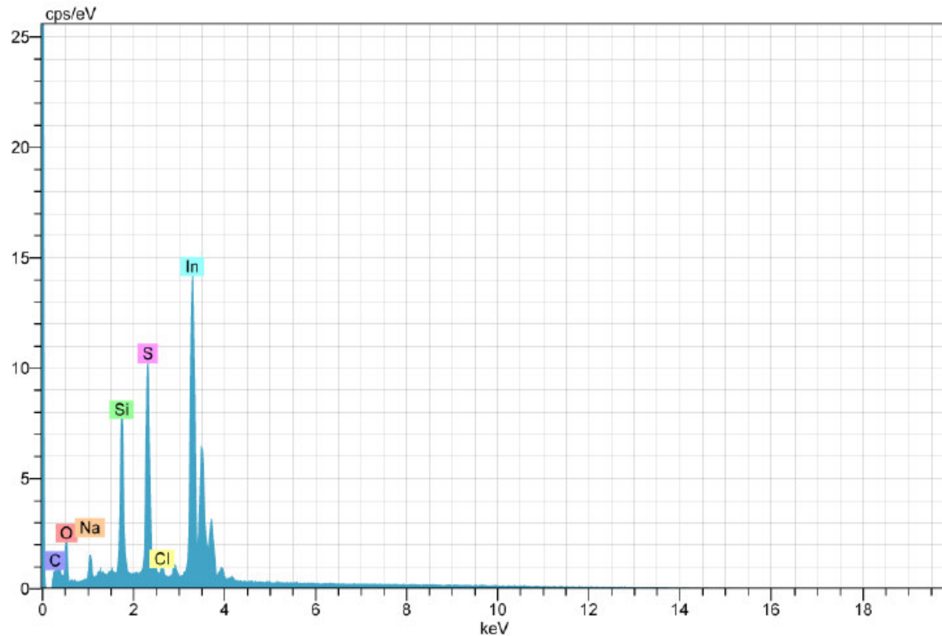

Figure 5.1 EDX spectra of the In_2S_3 film prepared by spray pyrolysis

Here, it is noticed that the content of sodium (Na) and silicon (Si) for In_2S_3 films deposited on glass substrate show the lower value, especially for the content of Na. Generally, glass substrate includes a lot of Na element, which is very active especially at high temperature so that Na element is easier to diffuse into In_2S_3. Furthermore, Na, as column element, will become acceptor if it substitutes indium position. In fact, Park et al. [102] have calculated that the position of the Na defect energy relatively to the valence band maximum amounts to 0.17 eV. Therefore, the In_2S_3 films prepared by spray pyrolysis had nearly stoichiometry.

5.3 XRD Studies

The as-grown In_2S_3 films deposited at different substrate temperatures were characterized by the XRD technique scanned in the 2-theta range of 20-50 degree. The diffractograms indicating the presence of all the prominent peaks of In_2S_3 are arising from (109), (220) and (309) reflections from the all In_2S_3 films that are polycrystalline having cubic structure. From Fig. 5.2, it is observed that the featureless spectra of the films deposited at substrate temperatures 200 ^{o}C reveal that the films possess amorphous structure whereas the presence of peak in the (220)

direction of the film deposited at higher substrate temperature 350 ^{o}C reveals that the film is crystalline in nature. And also it is observed that the XRD patterns of all In_2S_3 films show a most preferred orientation along (220) plane.

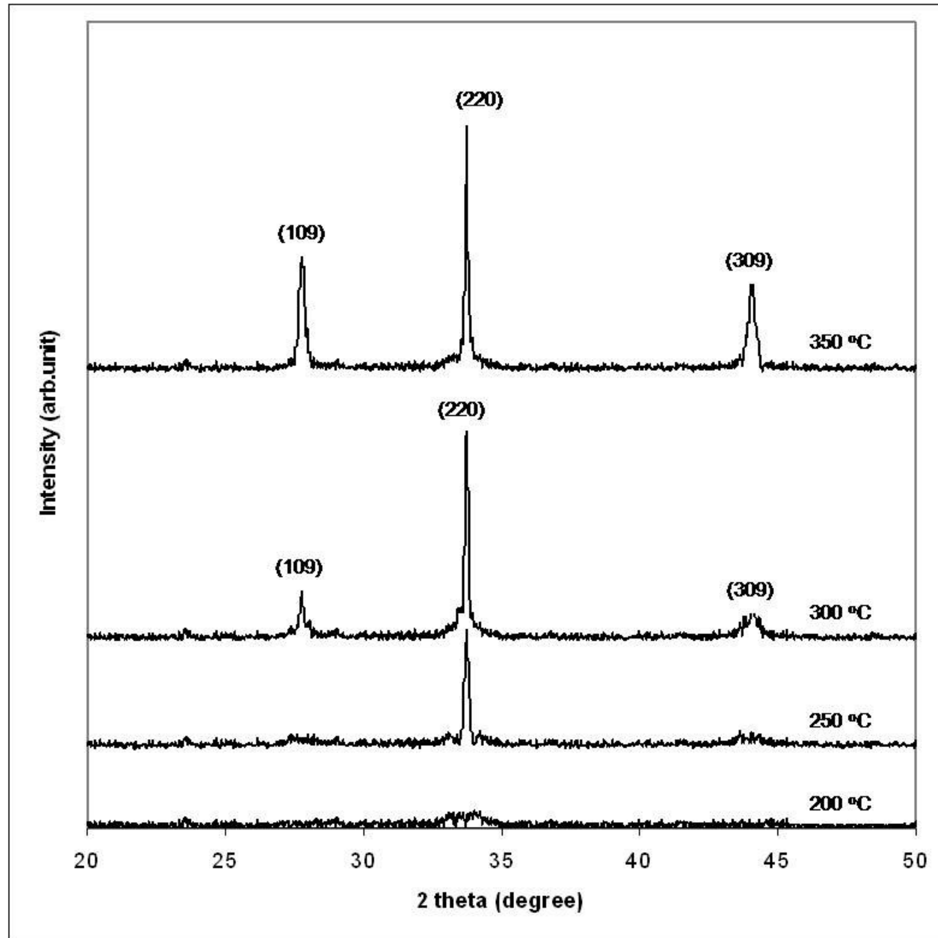

Figure 5.2 X-ray diffraction patterns of In_2S_3 films grown at different substrate temperatures, 200 ^{o}C, 250 ^{o}C, 300 ^{o}C and 350 ^{o}C

As the substrate temperature increased the peak intensities increased up to 350 ^{o}C, indicating the formation of more crystallites with well-defined orientation (220). The intensity of the (220) peak and its narrowing with an increase in the substrate temperature up to 350 ^{o}C indicated an improvement in the degree of crystallinity of the films. At 250 ^{o}C, In_2S_3 (220) peak is observed and this increases as the substrate temperature increases. Other peaks such as (109) and (309) are also observed in the films deposited at higher substrate temperatures and they increase as the substrate temperature increases. These results indicate that the crystallinity is improved in the

films deposited at higher substrate temperatures. This is in agreement with the results observed by Masahiro et al.[103]. As the substrate temperature increases, stronger and sharper diffraction peaks were observed. This was thought to result mostly from the grain growth, which released strains, and partly from homogenization, which increased the amounts of the stable phases present in the films.

Furthermore as the substrate temperature increases, gave rise to even stronger diffraction intensities for some diffraction peaks, namely, the In_2S_3 (220), (309) and (109). Hence, it can be assumed that the higher substrate temperature enables the atoms to move to the stable sites, which implies that films fabricated at these conditions are rather homogenous, and their crystalline state improves when the substrate temperature increases. It is concluded that the increase of the intensity of the XRD signal by increasing the substrate temperature can be explained by the crystallization of amorphous In_2S_3, formed beside crystalline In_2S_3 during deposition and increase in crystal size as seen from the decrease of the full width half maximum (FWHM). Therefore, the X-ray diffraction patterns give the most positive evidence of the formation of In_2S_3 phase, which was desired.

Hence, the dependence of the In_2S_3 film growth mechanism on substrate temperature can be explained on the basis of the reactions associated with the spray pyrolysis deposition process. Three possible film growth mechanisms, as a function of substrate temperature, explain the growth of In_2S_3 films with different properties in the present work. In the first case, the sprayed droplets impinge on the substrate kept at a low temperature of 250 ^oC, which is not sufficient to initiate reaction in the droplet. Films with foggy nature are formed. In the second stage, 300 ^oC is enough to make precipitates in the droplets and the solvent is evaporated just prior to touching the heated substrate, which initiates the decomposition of the sulphide. At the substrate temperature 350 ^oC (third stage), a sustained thermal reaction is taking place in which the film formation mechanism is associated with the volatilization of the precipitated indium salt and diffusion of the resulting vapour to the heated substrate, followed by its decomposition to the In_2S_3 film. No residues or powdery formation is observed. It is found that as the substrate temperature increases, crystallinity also increases. Relatively, higher peak intensities have been observed for the films deposited at 350 ºC. The decrease in XRD peak intensities with an increase

in the substrate temperature may be due to the sufficient increase in supply of thermal energy for recrystallization and the grain growth with temperature. Further decrease in crystallinity after 350 ºC may be attributed to the non-uniformity of the films. It is obvious that the growth of the In_2S_3 film samples is very dependent on the substrate temperature.

The values of particle size, strain and dislocation density for the films of different substrate temperatures are shown in Table 5.1.

Table 5.1 Structural parameters of In_2S_3 films at various substrate temperatures

Substrate temperature (^{o}C)	Grain size (nm)	Band gap (eV)	Dislocation density δ ($x10^{15}$ lin/m^2)	Strain ($x10^{-3}$lin^{-2}m^{-4})	Lattice constant a ($x10^{-10}$ m)	Lattice spacing d ($x10^{-10}$ m)
250	15.25	2.71	2.25	3.12	6.88	3.82
300	18.12	2.66	1.77	2.21	6.81	3.77
350	22.68	2.61	1.25	1.66	6.77	3.74

As seen in Table 5.1, the size of the crystallites oriented along (220) plane is calculated using Scherrer's Formula corresponding to each substrate temperature, neglecting peak broadening due to residual stresses in the films, $D=0,9\lambda/(\beta\cos\theta)$ where D is the size of crystallite, β is the broadening of diffraction line measured at half its maximum intensity in radians and λ is wavelength of X-ray (1,5405 A). The calculated values of crystallite size are given in the Table 5.1.

It has been observed that the crystallite size value increases with the increase of substrate temperature which may be due to decrease in strain value. Moreover, the increase of crystallite size with the growth temperature could be attributed to the improvement in the mobility of surface ad-atoms and an increase in the cluster formation leading to agglomeration of small grains. These agglomerated grains coalesce together resulting in the formation of larger grains with better crystallinity. Such an increase of particle size with increase of substrate temperature has also been reported by Masahiro et al. [103]. The dislocation density decreases with the increase

of substrate temperature. Since dislocation density and strain are the manifestation of dislocation network in the films, the decrease in dislocation density indicates the formation of high-quality films at higher substrate temperatures [104]. This is possibly because of the fact that when the substrate is kept at higher temperature, the dislocations get more thermal energy and have a higher mobility. The lattice constant decreased from 6.88 Å to 6.77 Å as the substrate temperature increased and showed a minimum value at a temperature of 350 ^{o}C indicating an improvement in the crystallinity with less defects and strain. The change in the lattice constant for all the films indicated that the grains are strained at lower and higher temperatures. This indicated that the optimum temperature to grow In_2S_3 films with less strain and defects was ~350 ^{o}C. Bender et al. also observed a reduction in the lattice constant with the increase of substrate temperature in the sputtered films [105]. The origin of lattice strain associated with chemically prepared films is related to the difference in the thermal expansion coefficients of the material to be deposited and substrate, and deviation from stoichiometry of the film that depends upon the deposition conditions [106]. Table 5.1 also gives the variation of the internal strain with substrate temperature, which indicated a reduction in the strain with the increase of deposition temperature. The change of crystallite size and lattice strain with substrate temperature could infer that higher the lattice strain, the lower will be the crystallite size. This implies that lattice strain in the films restricts the growth of grains. Ghosh et al. observed similar results for the ZnO films grown by sol–gel process [107]. And the grain size of the films increased from 15.25 nm to 22.68 nm with the increase of substrate temperature from 250 ^{o}C to 350 ^{o}C. The smaller grain size at low substrate temperature was due to poor crystallinity of the films.

As the substrate temperature increased, the crystallinity of the films was also improved. The crystallite size of In_2S_3 can be influenced by factors such as defects, impurities, and heating conditions. In case of the film, the role of substrate temperature is also very important because they can limit the growth direction and rate. It is found that although the data are scattered, there exists a trend of the crystallites to decrease in size with increase in strain. This may come from the retarded crystal growth due to the stretched lattice that can increase the lattice energy and diminishes the driving force of the growth. It is also showed that increase in grain size as a function of the substrate temperature is a consequence of the larger

mobility of the atoms at high temperature; thus, there is a decrease in the density of nucleation centers, and under these circumstances a smaller number of centers start to grow. It is concluded that the polycrystalline In_2S_3 film can be grown highly oriented along the (220) direction by spray pyrolysis technique.

5.4 Optical Characterization

Optical absorption studies of In_2S_3 films deposited on the glass substrates were carried out in the wavelength range of 300–900 nm at room temperature. The optical transmission spectra of the films prepared at different temperatures are shown in Figure 5.3.

A weak change in the absorption edge is observed towards higher wavelengths as T increases. The samples deposited at 250 ºC substrate temperature exhibit low transmittance. The reason may be attributed to the fact that the solution droplets form solid phase by evaporation only on reaching the surface of the substrate. It is observed that the transmittance of films increased as the substrate temperature increased.

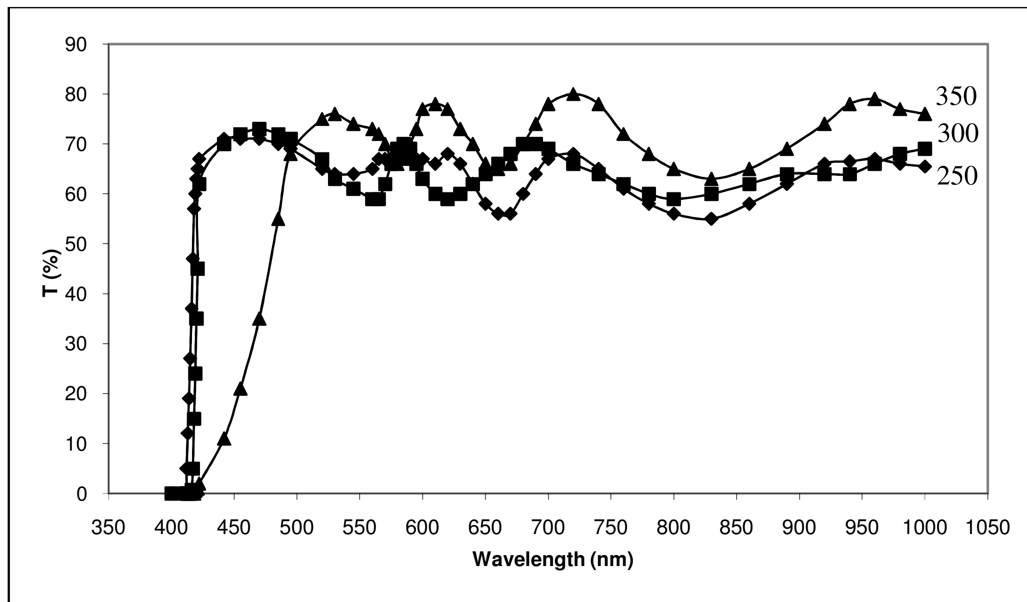

Figure 5.3 Optical transmittance T(%) spectra of In_2S_3 films deposited at different temperatures

This can be attributed to increasing grain size and roughening. This may also due to the arrangement of crystallites or grains. It indicates that substrate temperature is the most important factors influencing the film property. Thus, the higher transmittance observed in the films was attributed to less scattering effects, structural homogeneity and better crystallinity, whereas the observed low transmittance in the layers might be due to the less crytallinity leading to more light scattering.

A similar curve like in Fig. 5.4 can be obtained plotting the linear extrapolation of $(\alpha h\nu)^2$ versus $h\nu$ for thin film sample.

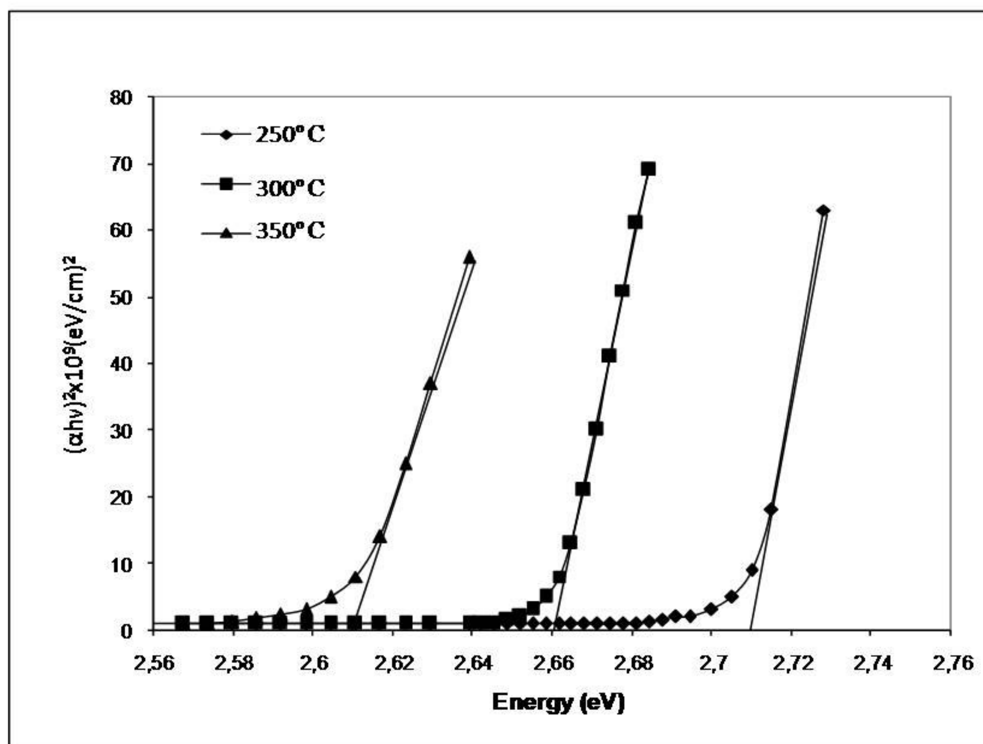

Figure 5.4 $(\alpha h\nu)^2$ versus $h\nu$ for In_2S_3 films deposited at different substrate temperatures, 250 °C, 300 °C and 350 °C

As the deposition temperature is increased from 250 ºC to 350 ºC, the band gap energy is decreased from 2.71 eV to 2.61 eV. The optical band gap of In_2S_3 film is obviously affected by the defects and the crystallinity. In general, there are several factors that influence the band gap of films. These include the band filling effect, quantum size confinement where the band gap increased with the decrease of grain

size, charged impurities at the grain boundaries, lattice strain present in the films and the extent of structural disorder. The analysis of the results in the present study suggested that there is a decrease of structural disorder in the films with the increase of substrate temperature from 200 ºC to 350 ºC, probably due to a reduction of defects at the grain boundaries of the layers that decreased the band gap.

Moreover, the decrease of the lattice strain in the films with growth temperature might also have contributed to the decrease of energy band gap in the present study. As the films were deposited at higher temperature, the crystallites began to move and tended to agglomerate easily. As a result, the band gap of crystallites decreases with increasing substrate temperature, which indicates that crystallization would cause the E_g narrowing. It could be explained by crystalline state improvement with increasing the substrate temperature. Also, the shift observed at absorption edge toward lower photon energies for the films deposited on heated substrates could be attributed to the increase in crystallite size and change in the stoichiometry. From the results of structure analysis, it is apparent that the optical band gap decreases with the decrease in defects and with the increase in grain size. This can be explained by the fact that free electrons are trapped in the defects and the grain boundaries. The density of defects decreases with the increase in deposition temperature and the density of grain boundaries decreases when the grain size increases at higher deposition temperature. It is observed that the substrate temperature mostly affects the band gap of the films.

5.5 SEM Analysis

The surface morphology of In_2S_3 films was analysed by using SEM. SEM images of In_2S_3 films are shown in Fig. 5.5(a, b, c, d). It is observed that the In_2S_3 film is homogenous, without cracks or pinholes and it well covers the glass substrate. In_2S_3 films deposited onto glass substrates with different substrate temperatures were used for study of surface morphology. Fig. 5.5 (a, b, c, d) shows SEM micrographs of In_2S_3 films onto glass substrates for 200, 250, 300 and 350 ºC substrate temperatures, respectively. Increase in substrate temperatures shows a substantial granular growth with increase of grain size. Increase in overgrowth of surface particles with temperature is well known for spray pyrolysis deposited films and is attributed to the process of precipitation with substrate tempereture. From these micrographs series a

noticeable effect of the temperature on the grain size can be observed. This result is a consequence of the higher time deposition time and amount of available material during the growth of thicker films. The film crystallite size depends on film deposition temperature. When the deposition begins, there are many nucleation centers on the substrate and small crystallites are produced. The films are deposited for only a low substrate temperature, the small crystallites on the substrate are not able to grow into large crystallites, and therefore the thinner (film of the thickness is less than 1μm) films have smaller crystallites than the thicker (>1μm) films. With increasing film deposition temperature, the crystallinity of the films is improved and the crystallite sizes become larger. This result is consistent with the XRD observation. In general, the grain shape and size change with the film deposition temperature, although a meticulous observation, allows us to see as the large grains present in higher deposition temperatures are formed by smaller ones. It was observed that the SEM of the In_2S_3 films (Fig. 5.5a) exhibit uniform surface, indicating its amorphous like behavior. Then, the grain features protruding from the film surface are enhanced with increasing film deposition temperature.

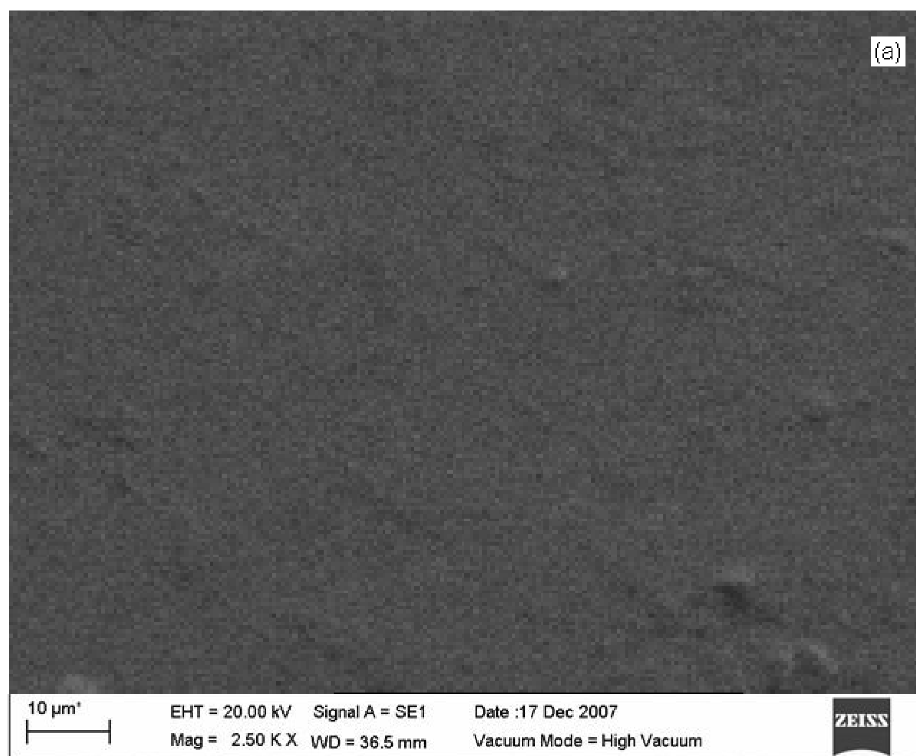

Figure 5.5(a) SEM image of In_2S_3 films at temperature 200 ºC

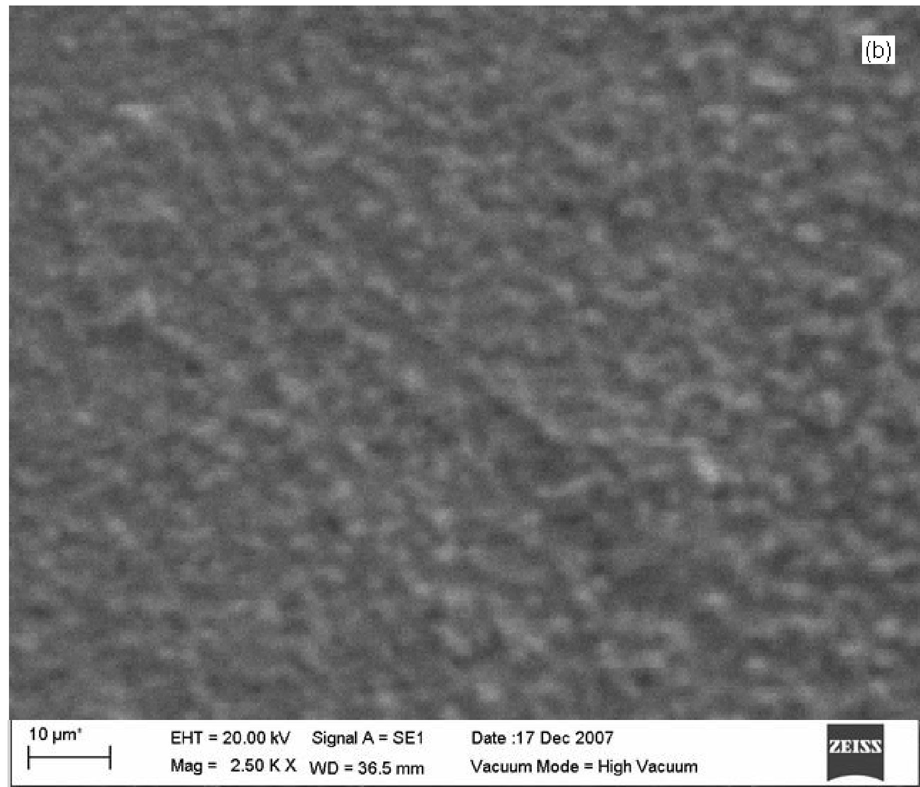

Figure 5.5(b) SEM image of In_2S_3 films at temperature 250 ºC

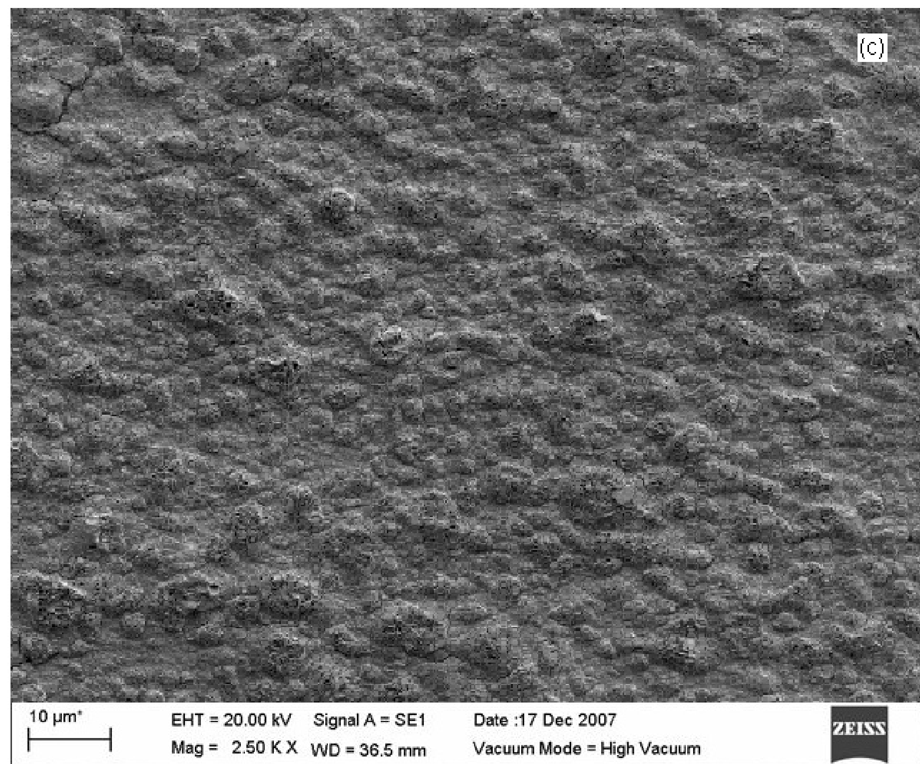

Figure 5.5(c) SEM image of In_2S_3 films at temperature 300 ºC

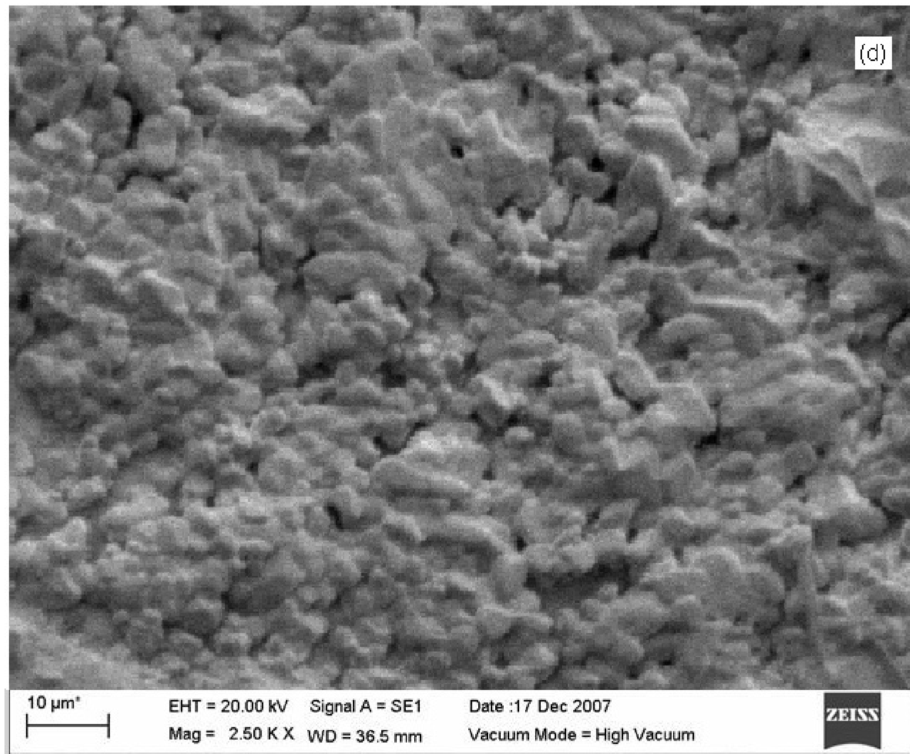

Figure 5.5(d) SEM image of In_2S_3 films at temperature 350 ºC

The grains are smaller and less definable producing smoother surface in micrograph of Fig. 5.5b, and larger and evenly scattered in Fig. 5.5c. The crystallinity of the film is evident from the spherical grains observed in Fig. 5.5c. This may be attributed to the polycrystalline nature of In_2S_3 film which provides nucleation sites and enhances the crystalline quality of films. In Fig. 5.5d, the grains were observed to have agglomerated together and formed smaller number of bigger grains. Also, in the case of the Fig. 5.5d, the surface is composed of elongated grains, which show a clear tendency to form agglomerates.

In all cases, the grains are homogeneously distributed all over the substrate surfaces. Comparing the micrographs in Fig. 5.5, the film produced with higher substrate deposition temperature clearly exhibits profound grain features. This can be explained by the film structural evolution with substrate temperature, in which the grains grow with increasing film deposition temperature. The transformation from the uniform smooth amorphous-like film structure to the fine grain features, followed by the growth in the grains the films with increasing film deposition temperature as demonstrated in Fig. 5.5 can be attributed to the surface energy minimization during

the growth process to achieve thermodynamical equilibrium. As the growth proceeds, those grains with preferred growth direction survive due to surface tends to evolve towards a situation of low surface energy. This results in evolution of large grained columnar morphology from a much larger number of fine grains, which were originally nucleated on the substrate, and improved film texture. Lin et al.[108] studied ZnO films and also obtained similar results. In addition, the roughness values were very close to the morphologies of growing films. It can be seen that the roughness increased with the increase of crystal size and the degree of crystallinity.

5.6 Transformation from the In_2S_3 Film to In_2O_3 Film

In this study, we produced the In_2S_3 films on the glass substrates at fixed substrate temperature 350 ^oC by the spray pyrolysis technique using indium chloride and thiourea as precursors, and then In_2O_3 films were obtained by thermal oxidation of the In_2S_3 films at different annealing temperature in O_2 flow. After deposition, thermal oxidation of In_2S_3 films was carried out in an oxygen flow at different annealing temperature range of 200, 400, 600 and 800 ^oC for 2 hours.

The main difficulty in depositing high-quality In_2O_3 films lies on oxygen vacancies and In interstitials, which will cause the nonstoichiometry in the In_2O_3 films. To overcome this drawback, thermal oxidation method has been studied for the preparation of In_2O_3 films. It is well known that oxygen impurity is found as a background impurity in many materials because of its easily diffusing properties into crystal lattice during the production of samples prepared by spray pyrolysis method. The oxygen impurities are first physically adsorbed at the grain boundaries and on the surface of the In_2O_3 films. The presence of oxygen impurities aids in recrystallization of the In_2O_3 films during the production process. Therefore, the oxygen impurity can alter the microstructure and the grain size of the sprayed In_2O_3 films during the production process [108]. In view of the presence of inherent oxygen impurity in the In_2O_3 films deposited by spray pyrolysis method and the extreme difficulties involved in the sprayed In_2O_3 films on glass substrates, the thermal oxidation method of In_2S_3 films provides a simple and convenient method to produce In_2O_3 films with high optical properties.

Fig. 5.6 shows the XRD patterns of as-deposited In_2S_3 films and the oxidized In_2O_3 films annealed at different temperatures ranging from 200 ^oC to 800 ^oC. The XRD spectrum for the as-deposited In_2S_3 film indicates that a high quality In_2S_3 film with a cubic crystal structure has been obtained with a preferred (220) orientation. The sample annealed at 200 $^{\circ}C$ also shows the cubic In_2S_3 films. When the films are annealed at 400 ^oC, the XRD spectra show a mixed pattern of In_2S_3 and In_2O_3 peaks, indicating that the In_2S_3 has begun a transformation from In_2S_3 to In_2O_3. For the annealing temperature of 600 ^oC, a (222) In_2O_3 peak is clearly seen. Thus the XRD pattern for the sample annealed at T_a = 600 ^oC only consists of In_2O_3 diffraction peaks, indicating that the In_2S_3 was fully transformed to In_2O_3 with a cubic crystal structure.

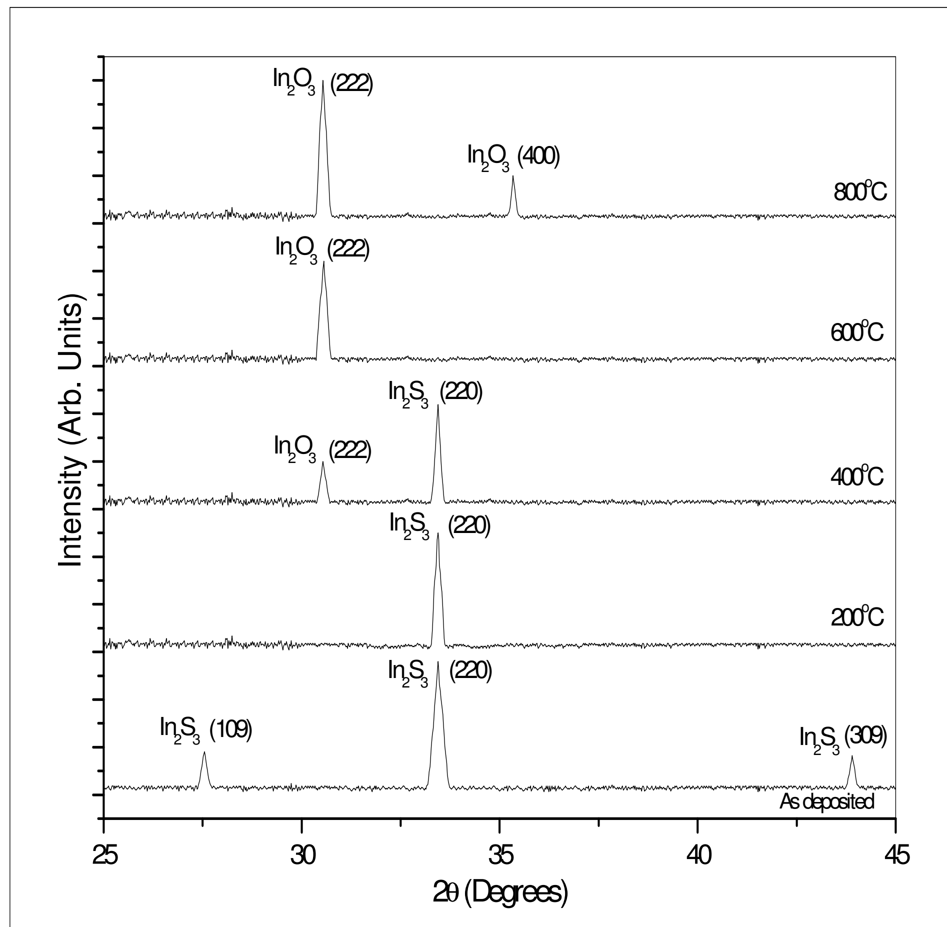

Figure 5.6 The XRD pattern of the as-deposited In_2S_3 films and the oxidized In_2O_3 films

For the samples annealed at $T_a \geq 600$ °C, only cubic In_2O_3 films was found in the XRD patterns, indicating the sulfur sites of cubic In_2S_3 films were replaced by oxygen during the thermal annealing process in O_2 flow. These results could be related that oxygen atoms diffuse into the In_2S_3 matrix via interstitial sites and bond to In, forcing sulfur atoms to occupy the interstitial sites in turn, leading to a modification of the cubic unit network. It is clearly seen from Fig.5.6 that the In_2O_3 film tends to grow in the directions (222) and (400). Therefore, the annealing processing makes the In_2O_3 film crystalline and denser. XRD pattern of crystallization phenomena is even significant with the elevation of temperature. When the temperature is continuously raised to 800°C, the crystallization is almost completely accomplished. Therefore, the crystallization of the film was even improved with the elevation of annealing temperature.

The grain size of the films was evaluated using the Debye-Scherrer formula [103]. The calculated average grain sizes are 39, 45 and 57 nm for the films annealed at temperature of 400, 600 and 800 °C, respectively. It is seen that the diffraction peaks of In_2O_3, such as (222) become sharper and more intense due to the increased particle size as well as the improved crystallinity as the annealing temperature increases.

The variation of the crystallite size of the preferred oriented peaks with respect to annealing temperatures is shown in Fig. 5.7**.**

It shows that in Fig.5.7, the crystallite size of the films is increased with increasing annealing temperature. The intense and sharp peaks in X-ray diffraction pattern reveal the good crystallinity of the films and also confirm the stoichiometric nature of In_2O_3 films. The single phase nature of the films was also confirmed from the presence of XRD peaks pertaining only to the In_2O_3 phase. With the increasing annealing temperatures the intensity of the diffracted peaks becomes more intense and sharp. The enhanced preferential orientation after annealing at high temperatures may be due to the movement of depositing atoms along the surface of the substrate to reach the low energy nucleation sites and growing preferentially there itself.

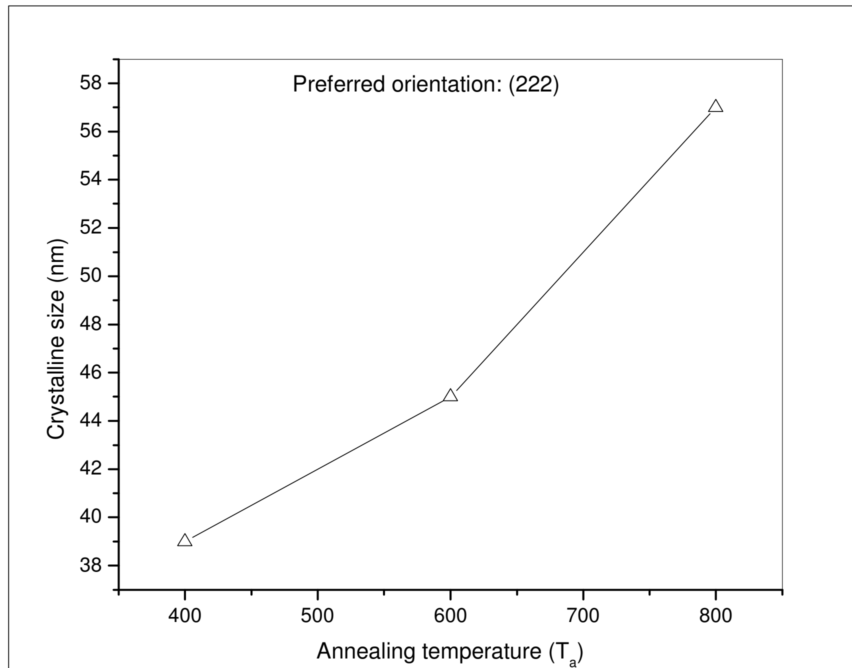

Figure 5.7 Variation in crystallite size of the In_2O_3 films with respect to annealing temperatures

Annealing temperature has an important effect on the transmittance and absorption edge. For the direct band-gap semiconductors, such as In_2O_3, the relation between the absorption coefficient α and the energy of the incident light $h\nu$ is expressed by Eq.4.8.

The values are near the bandgap energies obtained by Girtan et al. using the ultrasonic spray chemical vapor deposition [109]. The band gap energy of In_2O_3 films annealed at 600 ^oC is 3.68 eV. It shifts to 3.44 eV for samples annealed at 800 ^oC. Therefore the absorption edge shifts towards longer wavelength with increasing the annealing temperature and the absorption edge shifts gradually toward the longer wavelength, forming the band-gap shrinkage. It can be ascribed to the quantum confinement effect in nanocrystal materials. And the shift shrinkage in the evaluated optical energy band gap values towards the increasing annealing temperature may be due to the optical band filling effect that reveals the crystallization of the films.

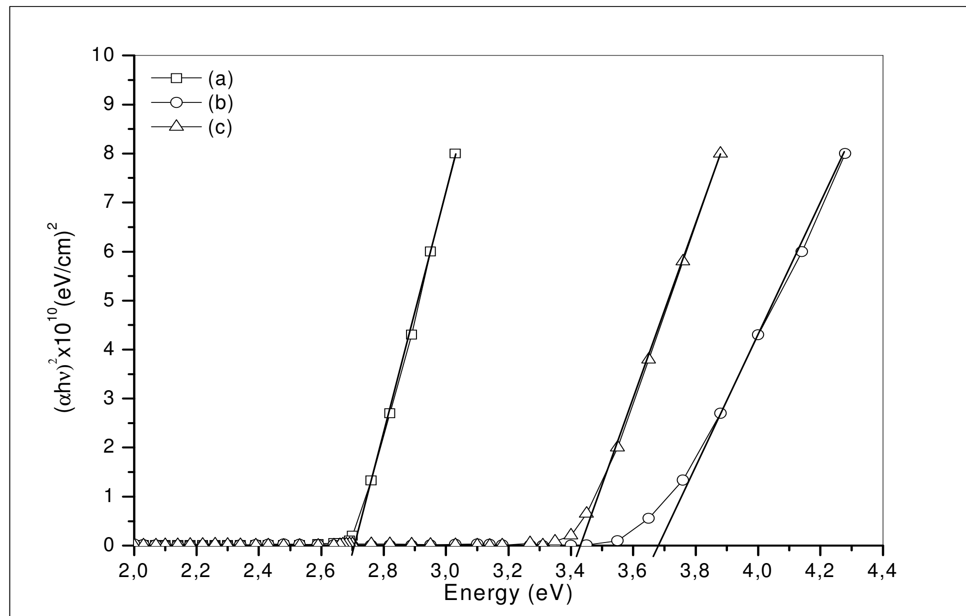

Figure 5.8 The plot of the $(\alpha h\nu)^2$ vs. the photon energy ($h\nu$) for (a) as-deposited In_2S_3 films and the oxidized In_2O_3 films at (b) 600 °C, (c) 800 °C

Furthermore the In_2O_3 film, which is annealing at 800 °C exhibits a high optical transmittance (greater than 90%). And the average optical transmittance increases with increasing the annealing temperature.

The increase in the optical transmittance is attributed to the well adherent and crystallized nature of the film throughout the coated area, which is obtained due to uniform thermal oxidation and improvement in lattice arrangement. And the increase in transmittance with higher annealed temperature may be due to decreasing optical scattering caused by the densification of grains followed by grain growth and the reduction of grain boundary density. In addition, the sharp absorption edge revealed at a wavelength of about 340 nm, which is very close to the energy bandgap of In_2O_3 (3.68 eV), implies the films possess good crystal quality. At 800 °C, the optical transmittance at wavelength of 340 nm can all reach up to 90%. The defect density inside the films gradually decreased with the increase of annealing temperature, and the crystalline of the films was also improved. It is known that the annealing treatment process can increase the homogeneity and crystallinity of the structure of the thin films and decrease the defect density at the edge of energy band gap. These

features suggest that a good quality In_2O_3 films with enhanced optical properties can be produced from the oxidixed In_2S_3 films.

CHAPTER 6

6. CONCLUSION

The XRD diffractograms indicating the presence of all the prominent peaks of In_2S_3 are arising from (109), (220) and (309) reflections from the all In_2S_3 films which are polycrystalline having cubic structure. The diffractograms depict that the deposits are polycrystalline for all the substrate temperatures. And also it is observed that the XRD patterns of all In_2S_3 films show a most preferred orientation along (220) plane. As the substrate temperature increased, the peak intensities increased up to 350 ºC indicating that the partial decomposition may be taking place, giving rise to a decrease in intensity. The intensity of the (220) peak and its narrowing with an increase in the substrate temperature up to 350 ºC indicated an improvement in the degree of crystallinity of the films.

The density of defects decreases with the increase in deposition temperature and the density of grain boundaries decreases when the grain size increases at higher deposition temperature. It is observed that the substrate temperature mostly affects the band gap of the films.

The EDX results taken from a dark area on the film show that the film contains small amounts of O, Na, and Si; these elements, are due to the elemental characteristics of the glass substrate. Carbon and Cl element are due to the $CS(NH_2)_2$ and $InCl_3$ solutions which were used as a source of sulphur and indium for the In_2S_3 film, respectively. Analytical results of EDX show that the ratio of In (indium) to S (sulphur) on the film was 55.61:44.39(at%).

As the deposition temperature was increased from 250 ºC to 350 ºC, the band gap energy is decreased from 2.71 eV to 2.61 eV. The optical band gap of In_2S_3 film is obviously affected by the defects and the crystallinity. The results of structure analysis, it is apparent that the optical band gap decreases with the decrease in defects and with the increase in grain size. As a result, the band gap of crystallites decreases with increasing substrate temperature, which indicates that crystallization

would cause the E_g narrowing. It could be explained by crystalline state improvement with increasing the substrate temperature.

A good quality In_2O_3 films have been successfully prepared by the thermal oxidation of the In_2S_3 films in air. Films oxidized at 600 ^oC reveal a cubic crystal structure with a preferential *c*-axis (222) orientation and no In_2S_3 phase was detected, indicating that the as-deposited In_2S_3 films have transformed to the In_2O_3 films completely. The band gap energy shifts from 3.68 to 3.44 eV when the films were annealed at 600–800 ^oC. Also with increasing the annealing temperature from 600 ^oC to 800 ^oC, the absorption edge is shifted to longer wavelength and accordingly the band gap energy decreases. It indicates that the oxygen in the annealing atmosphere has significant effects on the structure and optical properties of In_2O_3 films. Therefore, the In_2O_3 films prepared by thermal oxidation of In_2S_3 films are a promising candidate for optoelectronic and photovoltaic devices.

REFERENCES

[1] Kher S.S., Wells R.L. (1994) *Chem. Mater*. **6**:2056.

[2] Cui Y., Wei Q., Park H., Lieber C.M. (2001) *Science,* **293**:1289.

[3] Cui Y., Lieber C.M. (2001) *Science*, **291**:851.

[4] Chopra K.L., Major S., Pandya D.K. (1983) *Thin Solid Films* **102**:1.

[5] Granquist C.G. (2000) *Sol. Energy Mater. Sol. Cells.,* **60**:2301 .

[6] Kane J., Schweizer H.P. (1975) *Thin Solid Films,* **29**:155 .

[7] Manifacier J.C., Szepessy L., Bresse J.F., Peroten M., Stuck R. (1979) *Mater. Res. Bull.*, **14**:109.

[8] Naguchi S., Sakai H. (1980) *J. Phys. D*., **13**:1129.

[9] Murali K.R., Sambasivam V., Jayachandran M., Chockalingam M.J., Rangarajan N., Venkatesan V.K. (1988) *Surf.Coat. Technol.,* **35**:297.

[10] Haines W.G. (1978) Bube R.H., *J. Appl. Phys.,* **49**:304 .

[11] Seyam M.A.M., (2001) *Optical and electrical properties of indium monosulfide (InS) thin films*. Vacuum, **63**:441-447.

[12] Hara K., Sayama K., and Arakawa H. (2001) Semiconductor-sensitized solar cells based on nanocrystalline In_2S_3/In_2O_3 thin film electrodes. *Sol. Energy Mater. Sol. Cells,* **62**:441-447.

[13] Shay J.L., Tell B. (1973) Energy band structure of I–III–VI_2 semiconductors. *Surface Science,* **37**:748-762.

[14] George J., Joseph K.S., Prodeep B., Pulson T.I. (1988) Reactively evaporated films of indium sulphide Phys. Status Solidi, *Appl. Res.,* **106**:123.

[15] Barreau N., Bernède J.C., Marsillac S., Amory C., Shafarman W.N. (2003) New Cd-free buffer layer deposited by PVD: In_2S_3 containing Na compounds, *Thin Solid Films.*, **431**:326-329.

[16] Bube R.H., and McCarroll W.H. (1959) Photoconductivity in indium sulfide powders and crystals, *Journal of Physics and Chemistry of Solids*. **10(4):**333-335.

[17] Yukawa T., Kuwabara K. and Koumoto K. (1996) Electrodeposition of $CuInS_2$ from aqueous solution (II) electrodeposition of $CuInS_2$ film, *Thin Solid Films*, **286**:151-153.

[18] Belgacem S., Amlouk M., Bennaceur R. (1990) The Effect of Cu/In Ratio on the Structure of Thin Films of CuInS2 Made By Airless Spraying. (In French.). *Rev*

Phys Appl. **25(12)**:1213-1223.

[19] Kazuki I.M., Nakamura T.A., Arai E. (2001) Photochemical deposition of Se and CdSe films from aqueous solutions. *Thin Solid Films*. **384**:157-159.

[20] John T.T., Bini S., Kashiwaba Y., Abe T., Yasuhiro Y., Kartha C.S., Vijayakumar K.P. (2003) Characterization of spray pyrolysed indium sulfide thin films, *Semiconductor Sci. Technol*. **18**:491.

[21] Kumaresan R., Ichimura M., Sato N., Ramasamy P. (2002) Application of novel photochemical deposition technique for the deposition of indium sulfide. Mater. Sci. Eng., *B. Solid-State Mater. Adv. Technol.* **96**:37-42.

[22] Kamoun N., Bennaceur R., Amlouk M., Belgacem S., Mliki N., Frigerio J.M., Theye M.L. (2000) Structural and Photoelectrical Properties of Sprayed β-In_2S_3 Thin Films, *Physica Status Solidi (a),* **181(2)**:427-435.

[23] Bouguila N, Bouzouita H, Lacaze E, Amara A B,Bouchriha H, Dhouib A. (1997) *Effet de la température de fabrication sur les propriétés structurales et morphologiques des couches épaisses de In_2S_3 "spray"* .J Phys III Fance. **7(8)**:1647-1660.

[24] Naghavi N., Henriquez R., Laptev V. (2004) Lincot D. Growth studies and characterisation of In_2S_3 thin films deposited by atomic layer deposition (ALD). *Applied Surface Sci.* **222**:65-73.

[25] Asikainen T., Ritala M., Leskelä M. (1994) Growth of In_2S_3 thin films by atomic layer epitaxy. *Applied Surface Sci.* **82/83**:122-125

[26] George J., Joseph K.S., Pradeep B., Palson T.I. (**1988)** Reactively evaporated films of indium sulphide. *Physica status solidi (a)*. **106(1):**123-131.

[27] El Shazly A.A., Abd Elhady D., Metwally H.S., Seyam M.A.M. (1998) Electrical properties of β-In_2S_3 thin films. *Journal of Physics: Condensed Matter*. **10(26)**:5943.

[28] Guillén C., García T., Herrero J., Gutiérrez M.T. (2004) Briones F. Tailoring growth conditions for modulated flux deposition of In_2S_3 thin films. *Thin Solid Films.* **451/452**:112-115.

[29] John T.T., Mathew M., Sudha Kartha C., Vijayakumar K.P., Abe T., Kashiwaba Y. (2005) *Sol. Energy Mater. Sol. Cells*. **89**:27.

[30] Herrero J., Ortega J., (1988) *Sol. Energy Mater.* **17**:357.

[31] Kim W.T., Kim C.D., (1986) *J. Appl. Phys.* **60**:2631.

[32] Nomura R, Konishi K, Matsuda H. (1990) *Thin Solid Films* **198**:339.

[33] Sobolev A.B., Chaparro A.M., Gutiérrez M.T., Herrero J., Maffiotte C., (2004) *Electrochim. Acta*, **49** 737.

[34] Asenjo B., Chaparro A.M., Gutiérrez M.T., Herrero J., Maffiotte C. (2005) *Thin Solid Films*, **480–481**:151.

[35] Spiering S., Hariskos D., Powalla M., Naghavi N., Lincot D., Materials Research Society Spring Meeting, Strasburg 2002, B/ PIII.01., 2002.

[36] Kim WT, Kim CD. (1986) *J Appl Phys*. **60(7)**:2631.

[37] Kim WT, Yun CS. (1986) *J Appl Phys.* **60(7)**:2357.

[38] John T.T., Bini S., Sudha Kartha C., Vijayakumar K.P., Abe T., Kashiwaba Y., (2002) In: Proceedings of the international conference on recent advances in inorganic materials (RAIM-02). p. 106.

[39] Bhira L, Essaidi H, Belgacem S, Couturier G, Salardenne J, Barreaux N, et al. (2000) *Phys Stat Solidi (a)* **181**:427.

[40] Kamoun N., Bennaceur R., Amlouk M., Belgacem S., Mikli N., Frigerio J.M., et al. (1998) *Phys Stat Solidi (a)* **169**:97.

[41] Kamoun N., Belgacem S., Amlouk M., Bennaceur R., Bonnet J., Touhari F., et al. (2001) J *Appl Phys* **89(5):**2766.

[42] Amlouk M, Ben Said MA, Kamoun N, Belgacem S, Brunet N, Barjon D. (1999) *Jpn J Appl Phys* **38**:26.

[43] Hariskos D, Ruckh M, Ru¨ hle U, Walter T, Schock HW, Hedstro¨ m J, et al. (1996) *Sol Energy Mater Sol Cells* **41/42**:345.

[44] John T.T.,., Abe T., Kashiwaba Y., (2006) *Vacuum* **80**:870-875.

[45] A. Timoumi, H. Bouzouita, M. Kanzari, B. Rezig, (2005) *Thin Solid Films* **480-481**:124-128.

[46] Ratheesh Kumar P.M., John T.T.,, Sudha Kartha C, Vijayakumar K.P. (2006) *Nuclear Instruments and Methods in Physics Research B* **244**:171-173.

[47] Bini S., Kashiwaba Y., Abe T., Yasuhiro Y., Vijayakumar K.P. (2003) *Semicond. Sci. Technol*. **18**:491.

[48] John T.T., Mathew M., Sudha Kartha C., Vijayakumar K.P., Abe T., Kashiwaba Y., (2005) *Sol. Energy Mater. Sol. Cells* **89**:27.

[49] Gilbert-Mougel C., Couvreur F., Costantini J.M., Bouffard S., Levesque F., Hemon S., Paumier E., Dufour C. (2001) *J. Nucl. Mater.* **295**:121.

[50] Kamboj M.S., Kaur G., Thangaraj R., Avasthi D.K. (2002) J. Phys. D: *Appl. Phys.* **35**:477.

[51] El-Nahass M.M., Khalifa B.A., Soliman H.S., Seyam M.A.M. (2006) *Thin Solid Films* **515**:1796-1801.

[52] Rampersadh N.S., Venter A.M., Billing D.G. (2004) *Physica B* **350**:383.

[53] El-Shazly A.A., Abd El Hady D., Metwaly H.S., Seyam M.A.M. (1998) J. Phys., *Condens. Matter* **10**:5943.

[54] Lokhande C.D., Ennaoui A., Patil P.S., Giersing M., Diesner K., Muller M., Tributsch H. (1999) *Thin Solid Films* **340**:18.

[55] Sandoval-Paz M.G., Sotelo-Lerma M., Valenzuela-Jauregui J.J., Flores-Acosta M., Ramirez-Bon R. (2005)*Thin Solid Films* **472**:5.

[56] Barreau N., Marsillac S., Bernede J.C., Barreau A. (2000) *Appl. Surf. Sci.* **161**:20.

[57] Barreau N., Bernede J.C., H. El Maliki, Marsillac S., Castel X., Pinel J. (2002) *Solid State Commun.* **122**:445.

[58] Mane R.S., Lokhande C.D. (2002) *Mater. Chem. Phys.* **78**:15.

[59] Naghavi N., Henriquez R., Laptev V., Lincot D. (2004) *Appl. Surf. Sci.* **222**:65.

[60] Barreau N., Bernede J.C., Marsillac S. (2002) *J. Cryst. Growth* **241**:51.

[61] Barreau N., Marsillac S., Albertini D., Bernde J.C. (2002) *Thin Solid Films* **403**:331.

[62] John T.T., Bini S., Kashiwaba Y., Abe T., Yasuhiro Y., Kartha C.S., Vijayakumar K.P. (2003) *Semicond. Sci. Technol.* **18**:491.

[63] Choe S.H., Bang T.H., Kim N.O., Kim H.G., Lee C.I., Jin M.S., Oh S.K., Kim W.T. (2001) *Semicond. Sci. Technol.* **16**:98.

[64] Guillen C., Garcia T., Herrero J., Gutierrez M.T., Briones F. (2004) *Thin Solid Films* **451-452**:112.

[65] Sandolaz-Paz M.G., Sotelo-Lerma M., Valenzuela-Jauregui J.J., Flores-Acosta M., Ramiez-Bon R. (2005) *Thin Solid Films* **472**:5-10.

[66] Canava B., Guillemoes J.F., Yousfi E.B., Cowache P., Kerber H., Schock A., Schock H.W., Powalla M., Ariskos D., Lincot D. (2000) *Thin Solid Films* **361–362**:187.

[67] Hariskos D., Powalla M., Chevaldonnet N., Lincot D., Schindler A., Dimmler B. (2000) *Thin Solid Films* **387**:179.

[68] Boyle D.S., Bayer A., Heinrich M.R., Robbe O., O'Brien P.O. (2000) *Thin Solid Films* **361– 362**:150.

[69] Kostoglu M., Andritsos N., Karabelas A.J. (2001) *Thin Solid Films* **387**:115.

[70] Nemec P., Nemec I., Nahalkova P., Knizek K., Maly P. (2002) *J. Cryst. Growth* **240**:484.

[71] Ortun˜o-Lo´pez M.B., Valenzuela-Ja´uregui J.J., Sotelo-Lerma M., Mendoza-Galva´n A., Ramı´rez-Bon R. (2003) *Thin Solid Films* **429**:34.

[72] Herrero J., Gutierrez M.T., Guille´n C., Don˜a J.M., Martı´nez M.A., Chaparro A.M., Bayo´n R. (2000) *Thin Solid Films* **361– 362**:28.

[73] Barreau N., Marsillac S., Albertini D., Bernede J.C. (2002) *Thin Solid Films* **403–404**:331.

[74] Hariskos D., Ruckh M., Ruhle U., Walter T., Werner Shock H., Hedstrom J., Stolt L. (1996) *Solar Energy Mater. Solar Cells* **41–42**:345.

[75] Spiering S., Hariskos D., Powalla M., Naghavi N., Lincot D. (2003) *Thin Solid Films* **431– 432**:359.

[76] Kim W.T., Kim C.D. J. (1986) *Appl. Phys.* **60** 2631.

[77] George J., Joseph K.S., Pradeep B., Palson T.I. (1988) *Phys. Status Solidi,* A **106**:123.

[78] Herrero J., Ortega J. (1988) *Solar Energy Mater.* **17**:357.

[79] Bayon R., Herrero J. (2000) *Appl. Surf. Sci.* **158**:49.

[80] Lockande C.D., Ennaoui A., Patil P.S., Giersig M., Diesner K., Muller M., Tributsch H. (1999) *Thin Solid Films* **340**:18.

[81] Powder Diffraction File, Joint Committee on Powder Diffraction Standards, ASTM, Philadelphia, PA, 1967, Card 250390.

[82] O'Brien P., Octway D.J., Walsh J.R. (1998) *Thin Solid Films* **315**:57.

[83] Hara K., Sayama K., Arakowa H. (2000) *Sol. Energy Mater. Sol. Cells* **62**:441.

[84] Mane R.S., Lokhande C.D. (2002) *Mater. Chem. Phys.* **78**:15.

[85] George J., Joseph K.S., Prodeep B., Pulson T.I. (1988) *Phys. Status Solidi, Appl. Res.* **106**:123.

[86] Yousfi E.B., Weinberg B., Donsanti F., Cowache P., Lincot D. (2001) *Thin Solid Films* **387**:29.

[87] Timoumi A., Bouzouita H., Brini R., Kanzari M., Rezig B. (2006) *Applied Surface Science* **253**:306-310.

[88] Blatt F.J.(1968). *Physics of Electronic Conduction in Solids.* McGraw-Hill Education.

[89] Kevin F. Brennan. *Introduction to Semiconductor Devices: For Computing and Telecommunications Applications,* Cambridge University Press.

[90] http://britneyspears.ac/physics/basics/basics.htm

[91] http://semiconductors.com.ru/

[92] http://en.wikipedia.org/

[93] Weller H. (1993) *Colloidal Semiconductor Q-Particles: Chemistry in the Transition Region Between Solid State and Molecules,* Angewandte Chemie International Edition in English,41-43.

[94]physuna.phs.uc.edu/suranyi/Modern_physics/Lecture_**Not**es/modern_physics**11**.html

[95] Afzaal M., O'brien P. (2006) *Recent developments in II-VI and III-VI semiconductors and their applications in solar cells,* Journal of Material Chemistry, **16**:1597-1602.

[96] Schlüter M. , Camassel J. , Kohn S. , Voitchovsky J. P. , Shen Y. R. , and Cohen M.L. (1976) *Optical properties of GaSe and* GaS_xSe_{1-x} *mixed crystals,* Phys. Rev. B **13**: 3534 - 3547.

[97] Timoumi A., Bouzouita H., Kanzari M. and Rezig B. (2006) *Eur. Phys. J. Appl. Phys.* **33**:77-81.

[98] Herrero J., Gutiérrez M. T., Guillén C., J. Doña M., Martínez M. A., Chaparro A. M. and Bayón R. (2000) *Thin Solid Films,* **361-362**:28-33.

[99] http://www.allaboutcircuits.com/vol_3/chpt_2/3.html

[100] http://www.siliconfareast.com/

[101] Pacific Northwest National Laboratory. *Scientists have Shown that a Chunk of Hematite Can Conduct Electrons Under Certain Chemical Conditions.* United States: Kevin Rosso.

[102] Park C.H., Zhang S.B., S.- Wei H. (2002) *Phys. Rev. B*, **66**:073202.

[103] Masahiro T., Narumi I., Yoshizumi Y. (1996) *Vacuum*, **47**:239.

[104] Chou L. H. (1992) *Thin Solid Films*, **215**:188.

[105] Bender M., Katsarakis N., Gagaoudakis E., Hourdakis E., Douloufakis E., Cimalla V., Kiriakidis G. (2001) *J. Appl. Phys.,* **90**:5382.

[106] Korotcenkov G., Brinzari V., Cerneavschi A., Cornet A., Morante J., Cabot A., Arbiol J. (2002) *Sens. Actuat. B*, **84**:37.

[107] Ghosh R., Basak D., Fujihara S. (2004) *J. Appl. Phys.,* **96**:2689.

[108] Oztas M., Yazici A.N. (2004) *J. Lumin.,* **110**:31.

[109] Girtan M. and Folcher G. (2003) *Surf. Coat. Technol.* 172 242.

PUBLICATIONS

[1] Öztaş M., Bedir M., Öztürk Z., Korkmaz D. and Sür S., " Structural and optical properties of nanocrystal In_2O_3 films by thermal oxidation of In_2S_3 films" , *Chinesee Physics Letter,* **23** 1610 (2006).

[2] Korkmaz D., " Investigations on In_2S_3 films" , *5th International Student Conference of Balkan Physical Union(ISCBPU5)*, 109, Bodrum (2007).